PNAS
www.pnas.org

Supplementary Information for

Bromodomain proteins regulate human cytomegalovirus latency and reactivation allowing epigenetic therapeutic intervention

Ian J. Groves[a]*, Sarah E. Jackson[a], Emma L. Poole[a], Aharon Nachshon[b], Batsheva Rozman[b], Michal Schwartz[b], Rab K. Prinjha[c], David F. Tough[c], John H. Sinclair[a1], Mark R. Wills[a*1]

[a]Cambridge Institute of Therapeutic Immunology and Infectious Disease and Department of Medicine, University of Cambridge School of Clinical Medicine, Cambridge Biomedical Campus, Cambridge, UK, CB2 2QQ.

[b]Department of Molecular Genetics, Weizmann Institute of Science, Rehovot, Israel

[c]Adaptive Immunity Research Unit, GlaxoSmithKline Medicines Research Centre, Stevenage, UK

[1]Authors contributed equally

*Corresponding authors: Ian J Groves, Mark R Wills.

Email: ijg25@cam.ac.uk, mrw1004@ cam.ac.uk

This PDF file includes:

Supplementary Methods

Cell culture. Peripheral blood mononuclear cells (PBMCs) were isolated from either peripheral blood or apheresis cones (NHS Blood and Transplant) by density gradient centrifugation (Lymphoprep, Axis-shield, Alere Ltd). HCMV serostatus was determined using serum from the sample and IgG levels analysed using an IgG enzyme-linked immunosorbent (EIA) assay (Captia HCMV IgG, Trinity Biotech) following manufacturer's instructions. CD14+ monocytes were then isolated by magnetic-activated cell sorting (MACS, Miltenyi Biotec) as per manufacturer's instructions using anti-CD14 magnetic beads, resulting cells being plated on plastic ware (5×10^5 per cm^2) for 3h in phosphate buffered saline (PBS) before washing twice and addition of X-Vivo-15 with 2mM L-glutamine (Lonza). Human foetal foreskin fibroblasts (HFFF) (ECACC, 86031405) were passaged in Dulbecco's modified Eagle's medium (DMEM) and THP-1 cells (ECACC, 88081201) in RPMI 1640 medium (Sigma), both supplemented with 10% heat-inactivated foetal bovine serum (FBS) (PAN Biotech), penicillin (100 U/ml) and streptomycin (100 µg/ml) (Sigma). All cells were incubated at 37 °C in a 5% CO_2 environment. Differentiation of CD14+ monocytes to macrophages was achieved with either: phorbol 12-myristate 13-acetate (PMA, 20nM) (Sigma)(1); or macrophage colony-stimulating factor (M-CSF, 20ng/ml) (Miltenyi Biotec) and interleukin-1β (IL-1β, 10ng/ml) (Miltenyi Biotec) for 4-days. Differentiation to mature DCs employed granulocyte-macrophage colony-stimulating factor (GM-CSF, 1,000 U/ml) (Miltenyi Biotec) and interleukin-4 (IL-4, 1,000 U/ml) (Miltenyi Biotec) for 5-days before the addition of lipopolysaccharide (LPS, 500 ng/ml) (Invivogen) for at least 2-days. THP-1-MIEP-eGFP cells (a gift from M. Van Loock, Johnson & Johnson (from which an isolated integrated HCMV MIEP expresses enhanced GFP upon differentiation)(2) and Kasumi-3 myeloblastic cells(3,4) were grown in RPMI 1640 medium (Sigma) supplemented with 20% heat-inactivated foetal bovine serum (FBS) (PAN Biotech), penicillin (100 U/ml) and streptomycin (100 µg/ml) (Sigma). The production and culture of human induced pluripotent stem (iPS) C2 cells has been described at length elsewhere(5). All cells were incubated at 37 °C in a 5% CO_2 environment and differentiation was achieved with PMA treatment (100nM; Sigma) for 48h.

Viruses and HCMV latent infection. TB40e-IE86-eYFP expresses the immediate early IE86 protein fused to enhanced YFP(6) and was derived with BAC vector (BAC4) insertion at US2-6 from a low passage wild type strain of TB40e(7). Due to the absence of a full complement of viral immune evasion genes in TB40e-IE86-eYFP, all experiments concerning immune analysis and requiring a fluorescent

marker were conducted with TB40e-UL32-GFP, which expresses the late protein pp150 (UL32 gene) fused to GFP(8). All viruses were a gift of Christian Sinzger (University of Ulm, Germany), have no growth deficits or attenuation and have been used previously(9). For experimental latent infection, CD14+ monocytes (pre-plated for 24 h) were incubated with virus at an MOI of ~5 (stock dependent) for 3 h at room temperature with rocking. Virus medium was then removed and cells were washed twice in PBS before replacing with X-Vivo-15 with 2mM L-glutamine and incubation for 5-days for transcriptional latency to ensue. For infection of THP-1 monocytes, cells were pre-cultured in RPMI with 2% FBS (RPMI-2) for 24 h before incubation with TB40e IE86-eYFP (MOI ~5) in suspension for 3 h with intermittent shaking. THP-1s were then washed twice in RPMI-2 medium before resuspension in RPMI-2 for 3-days for latency to establish. CD34+ cell lines were infected in suspension with HCMV TB40e IE86-eYFP at an MOI of ~5 (stock dependent) for 3 h at room temperature with agitation. Cells were washed twice in PBS before replacing medium and incubation for 3-days before treatment with compounds, DMSO (negative control) and PMA (100mM; positive control). YFP-positive cells were then counted per well and numbers normalised to PMA (set to 1).

HCMV reactivation analyses. CD14+ monocytes expressing fluorescent protein (green cells) after experimental infection with either TB40e-IE86-eYFP or TB40e-UL32-GFP and compound treatment were counted per well in comparison to DMSO background (negative control) and PMA (positive control) across various time courses. To determine if HCMV full reactivation had resulted, compound medium was withdrawn, cells washed and CD14+ monocytes overlaid with HFFF (3×10^4 per cm^2) in 50:50 mix of X-Vivo-15:DMEM-10 for between 7 to 14-days before green plaques were then counted. For HCMV latently infected killing experiments with T-cell co-cultures, lymphocytes were washed off before HFFF overlays were established and differentiation of CD14+ monocytes was used to produce green plaques to determine the remaining numbers of latently infected cells. Treatment of TB40e-IE86-eYFP latently infected THP-1 cells was carried out for 48 h before analysis of IE gene expression through YFP analysis relative to DMSO background (negative control) and PMA (positive control) via flow cytometry.

T-cell co-culture experiments. PBMC isolated from peripheral blood were depleted of either CD4+, CD8+ or total CD3+ T-cells by MACS using anti-CD4, anti-CD8 or anti-CD3 direct beads (Miltenyi

Biotec), respectively, according to manufacturer's instructions with separation using an AutoMACS Pro (Miltenyi Biotec). Efficiency of depletion was determined by staining a proportion of cells with a CD3-FITC, CD4-PE, and CD8-PerCP-Cy5.5 antibody mix (BioLegend) and analysis by flow cytometry with remaining cells amounting to no more than 1% of final co-culture. Lymphocyte co-cultures for HCMV latently infected killing experiments were established at an effector to target (E:T) cell ratio of 2:1.

HCMV lytic infection and compound treatment analysis. Human foetal foreskin fibroblasts (HFFFs) were treated with inhibitors for 16-hours before infection with HCMV TB40e IE86-eYFP (MOI experiment dependent). After 24h, cells were fixed with paraformaldehyde and nuclei counterstained with Hoechst before the number of YFP-positive cells and level of YFP expression per cell was assessed using ArrayScan technology, as well as the number of live cells by Hoechst stain relative to DMSO (negative control). For lytic DNA replication analysis, similarly pre-treated infected cells were cultured for 72h before DNA was harvested by the method described in the main methods section.

Epigenetic inhibitors and cytotoxicity. Cells were treated with epigenetic inhibitors provided by GlaxoSmithKline (Epigenetics toolbox) and commercially available inhibitors (see Table S1). Dimethyl sulfoxide (DMSO) was used to dissolve all compounds (stock at 10mM) and employed within experiments as a negative control. CDK9 inhibitor, Flavopiridol (FLAV) was used at 40nM and SEC inhibitor, KL-2 was used at 10μM as co-treatments with stated epigenetic inhibitors. Differentiation agents (see above) were used as positive controls throughout. To determine toxicity of compounds with CD14+ monocytes, plated cells were treated with compounds (30μM to 30nM) across a 96h time course before dead cells were stained with SYTOX orange (5μM in PBS) (Thermofisher), then fixed and nuclei counter-stained with Hoechst at individual timepoints. SYTOX-positive cells were then quantified using an ArrayScan (Thermofisher). For toxicity effects with THP-1 monoctyes, cells were treated with compounds (30μM to 30nM) for 48h before dead cells were stained with LIVE/DEAD Far Red Dead Cell stain kit as per manufacturer's instructions (Thermofisher) and then quantified on a BD Accuri C6 Plus flow cytometer (BD Biosciences).

Quantification of HCMV transcript level. RNA was isolated from plated CD14+ monocytes using RLT buffer and RNeasy Mini Kit (Qiagen), with quality and quantity being determined using a Nanodrop 1000

(Thermo), before elimination of genomic DNA and cDNA synthesis using 250ng of RNA with the Quantitect Reverse Transcription Kit (Qiagen). Relative transcript levels were then determined using HCMV cDNA-specific primers (Table S3) with Luna Universal SYBR Green qPCR Master Mix (NEB) as per manufacturer's instructions on an ABI StepOnePlus. Transcript levels were normalised for primer efficiency and referenced to host GAPDH transcript level using the Pfaffl method(10).

Quantification of HCMV DNA level by qPCR. DNA was isolated from CD14+ monocytes either experimentally or naturally infected with HCMV using a previously described method(11), with quality and quantity being determined using a Nanodrop 1000 (Thermo), before HCMV genomic DNA (gDNA) level was determined using HCMV gDNA-specific primers (Table S3) with Luna Universal SYBR Green qPCR Master Mix (NEB) as per manufacturer's instructions on an ABI StepOnePlus. DNA copy number was then determined by referencing to host GAPDH promoter copy number via the Pfaffl method(10).

Quantification of HCMV DNA level by digital droplet PCR (ddPCR). Latent HCMV carriage in epilepsy patients was carried out as described previously(9). Briefly, CD14+ monocytes were isolated from 20ml of heparinised peripheral blood before cells were counted and stored at -80°C before DNA extraction as per the protocol described in the main methods section. Measurement of HCMV DNA copy number was then carried out using ddPCR technology(11) whereby amplicons from PCRs using oligonucleotides directed at HCMV glycoprotein B (*gB*) or host gene *RPP30* produced in oil droplets were enumerated such that HCMV copy number could be calculated per 1 x 10^6 starting CD14+ cells.

Detection of HCMV protein expression by immunoblot. CD14+ monocytes were lysed with Laemmli buffer (Sigma) and samples separated by sodium dodecyl sulfate-polyacrylamide gel electrophoresis (SDS-PAGE) before transfer to nitrocellulose membrane. Protein expression was then determined in comparison to β-actin loading control using HCMV-specific primary and horseradish peroxidase (HRP) secondary antibodies (listed in Table S4) with enhanced chemiluminescence (ECL) Prime (Sigma).

Protein fractionation, semi-quantitative immunoblot analysis and indirect immunofluorescence. CD14+ monocytes isolated from apheresis cones were treated with HDACi (CHR-4487, 30nM), I-BET (GSK726, 30nM), PMA (20nM) or DMSO (equivalent concentration) for 24h before protein fractions (NE, nuclear extract; CE, cytoplasmic extract) were isolated from cells using the NE-PER Nuclear and Cytoplasmic Extraction (Thermofisher). Samples were then separated by SDS-PAGE and immunoblotted using specific antibodies for β-actin, histone H4 and CDK9 (Table S4) as per method in main text. The resulting bands were then semi-quantified using ImageJ densitometry compared to DMSO (set as 1), with CDK9 compared to β-actin and histone H4 as CE and NE loading controls, respectively. For indirect immunofluorescence analysis of CDK9 expression, equivalently compound treated CD14+ monocytes were fixed with 4% paraformaldehyde before permeabilisation with 0.1% TritonX-100 in PBS before labelling with CDK9-specific primary antibody and subsequent goat anti-rabbit AlexaFluor-488 secondary (see Table 4) with Hoechst nuclear counterstain. Cells were then viewed on a Nikon Eclipse TE300 microscope using a CoolLED pE-4000 platform.

Chromatin immunoprecipitation (ChIP) analysis. THP-1 cells (1×10^7 per condition) were incubated in RPMI with 2% FBS (RPMI-2) for 24h before infection in suspension with HCMV TB40e IE86-eYFP at an MOI of 5 (equivalent on HFFF) for 3h at 37 °C in a 5% CO_2 environment. Cells were then washed twice in PBS before resuspension in RPMI-2 and incubation for a further 3-days. Once HCMV latency had established, cells were separated into $15cm^2$ dishes and treated with compounds (DMSO, 30mM equivalent; CHR-4487, 30nM, GSK726, 30nM; PMA, 100nM) for 48-hours. Cells were then fixed, chromatin extracted, sonicated (using a Bioruptor Pico, Diagenode) and then immunoprecipitations carried out using the ChIP IT PBMC kit (Active Motif) as per manufacturer's instructions with ChIP validated antibodies (Table S4). Enrichment of target bound DNA was then quantified against isotype controls (set as 1) using HCMV gDNA-specific qPCR primers with ChIP verification through host control regions (Table S3).

Fluorospot analysis of cytotoxic T cell functionality. Fluorospot analysis of IFN-γ release from T cells treated with epigenetic inhibitors was carried out essentially as described previously(5). Briefly, pre-coated Fluorospot plates (Mabtech AB) were seeded in triplicate with 2×10^5 PBMC isolated by Lymphoprep centrifugation from the peripheral blood of both HCMV seropositive and negative

individuals with HCMV peptide mixes (IE72/IE86, UL83/pp65; 2µg/ml per peptide) or medium and positive control (CD3/CD28 stimulants; Mabtech AB) as well as epigenetic inhibitors: HDACi (CHR-4487, 30nM and 3nM) and I-BET (GSK726, 30nM and 3nM) in comparison to DMSO control (equivalent concentration). Plates were then incubated at 37 °C in a 5% CO2 environment. After 48h, cells and medium were removed from wells and the plates developed as per the manufacturer's instructions before being read on an AID iSpot reader (Oxford Biosystems) and the IFN-γ positive spots counted using the AID EliSpot v7 software (Autoimmun Diagnostika GmbH). All data was then presented as spot forming units (SFU) per 2 x 10^5 PMBC.

Myeloid cell phenotyping by flow cytometry. CD14+ monocytes isolated from apheresis cones were plated on plasticware for 24h before treatment (5 x 10^6 cells per condition) with HDACi (CHR-4487, 30nM and 3nM) and I-BET (GSK726, 30nM and 3nM) and PMA (20nM) in comparison to DMSO control (equivalent concentration) for a further 24h. In addition, monocytes were also treated for 6-days with GM-CSF/IL-4 (1,000 U/ml and 1,000 U/ml, respectively) for differentiation to dendritic cells (DCs) or for 4-days with M-CSF/IL-1β (20ng/ml, 10ng/ml, respectively) for differentiation to macrophage. At each endpoint, cells were removed from plasticware with cold PBS before blocking and then staining with either antibodies specific for surface markers associated with individual stages of myeloid differentiation, isotype control antibodies or unstained controls, as well as a live/dead cell stain in all cases (for reagents see Table S4). Samples were then fixed in 1% paraformaldehyde and stored in the dark at 4°C before processing on a Fortessa flow cytometer (BD Biosciences) using FACS Diva software. Samples were then analyzed using FlowJo software (Treestar, Oregon, USA), by using first a Time vs Side scatter gate, to identify the main flow of cells, then these cells were gated for single cells (Forward scatter area vs Forward scatter height), live cells (forward scatter width vs Live Dead Aqua dye), then monocyte/myeloid cells gate (Forward scatter area vs side scatter area (log scale)). Phenotype markers were analysed from this gate. The gating strategy for this phenotype panel was optimised using Fluorescence Minus One (FMO) controls in addition to the matching isotype control staining for each sample.

Cytotoxic T cell phenotyping by flow cytometry. To phenotype CD3+/CD4–/CD8– T cells, PBMC were isolated from peripheral blood of one HCMV seronegative and three seropositive individuals by

Lymphoprep gradient centrifugation. Cells were then stained with antibodies specific for natural killer cells (CD56), T cells (CD3/CD4/CD8 and α/β or γ/δ chains), as well as a live/dead cell stain in all cases (for reagents see Table S4), unstained controls and FMO controls were also prepared. Samples were then fixed in 1% paraformaldehyde and stored in the dark at 4°C before processing on a Fortessa flow cytometer (BD Biosciences) using FACS Diva software. Samples were then analysed using FlowJo software, by using first a Time vs Side scatter gate, to identify the main flow of cells, then these cells were gated for single cells (Forward scatter area vs Forward scatter height), live cells (forward scatter width vs Live Dead Aqua dye), then lymphocyte gate (Forward scatter area vs side scatter area (log scale)). CD4- CD8- T cells were gated from the lymphocyte gate and the expression of CD3, CD56 and TCR γ/δ were assessed.

YFP-positive cell sorting and RNA library construction. CD14+ monocytes latently infected with HCMV-TB40e-IE86-eYFP were treated with compounds (CHR-4487 30nM; GSK726 30nM; PMA 20nM; and DMSO equivalent dilution). After 72h, cells were released from plasticware using cold PBS and 10,000 YFP-positive cells per condition (from an initial 8 x 10^6) were FACS sorted directly into 40µl of lysis/binding buffer (Thermofisher) in Ultra High Recovery 1.5ml microcentrifuge tubes (Starlab). Samples were then vortexed and snap-frozen on dry ice and stored at -80°C. Library preparation for RNA-seq was then carried out essentially as per the massively parallel single-cell RNA-seq (MARS-seq) protocol(12) using reverse transcription (RT)-indexed poly(T) primers, which leads to libraries equating to the 3' end of HCMV and host mRNA transcripts.

Sequencing and data analysis. RNA-Seq libraries (pooled at equimolar concentration) were performed in duplicates and sequenced using NextSeq 500 (Illumina), with read parameters - Read1: 72 cycles and Read2: 15 cycles. Alignment and analysis were done as described previously(58). The number of Unique Molecular Identifiers (UMIs) were: 1,837,419 and 4,301,957 for the DMSO samples; 1,331,708 and 1,628,589 for the PMA samples; 754,441 and 980,506 for the CHR-4487 samples; and 729,659 and 430,720 for the GSK726 samples. The differential expression analysis was done with DESeq2 (version 1.22.2) using default parameters, with the number of reads in each of the samples as an input. HCMV transcript functional and temporal expression annotations are present in Table S2. All sequencing data is available online at GSE156169.

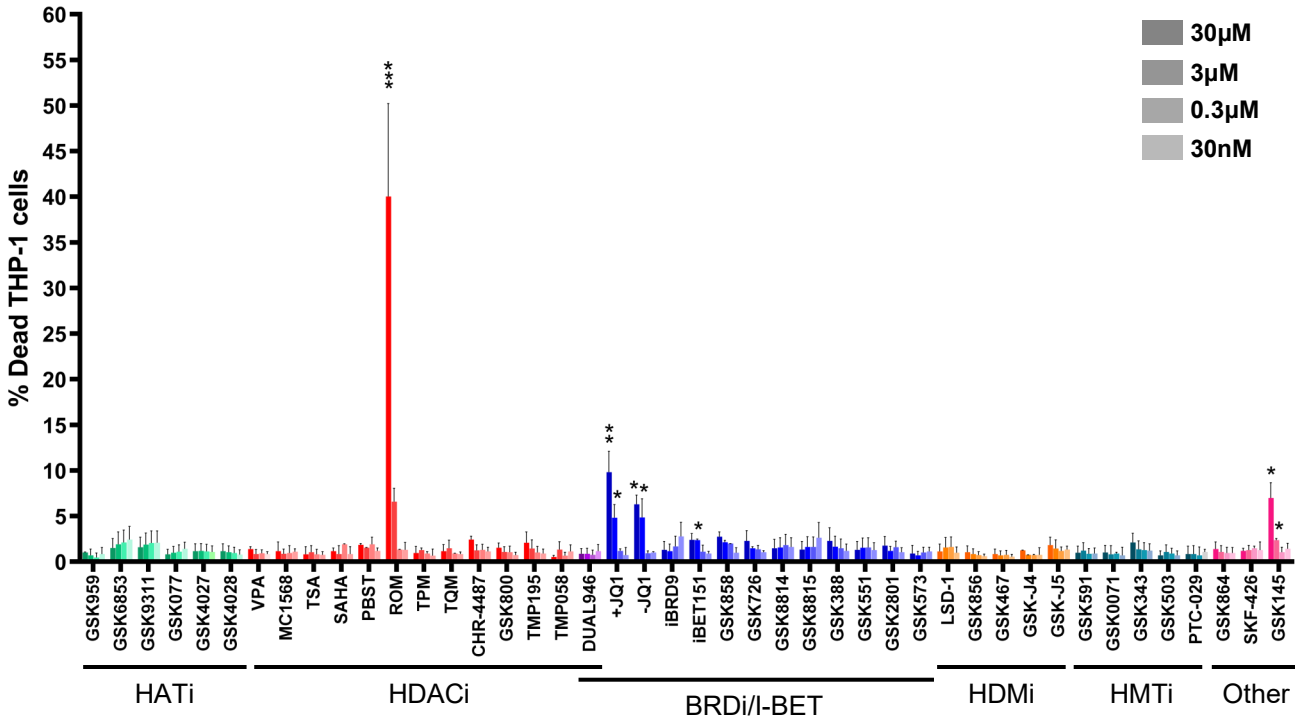

Figure S1. Toxicity of epigenetic modifier inhibitors in the THP-1 monocytic cell line. THP-1 monocytes were treated with inhibitors of histone acetyltransferases (HATi, green), histone deacetylases (HDACi, red), bromodomain proteins (BRDi/I-BET, blue), histone demethylases (HDMi, orange), histone methyltransferases (HMTi, teal) as well as other epigenetic modifiers (Other, pink) across a range of concentrations (30-0.3μM) for 48 hours. Cells were then stained with live/dead stain and analysed by flow cytometry in comparison to DMSO (negative control). *n* = 3; bars = mean +SEM. **P*<0.05, ***P*<0.01, ****P*<0.001.

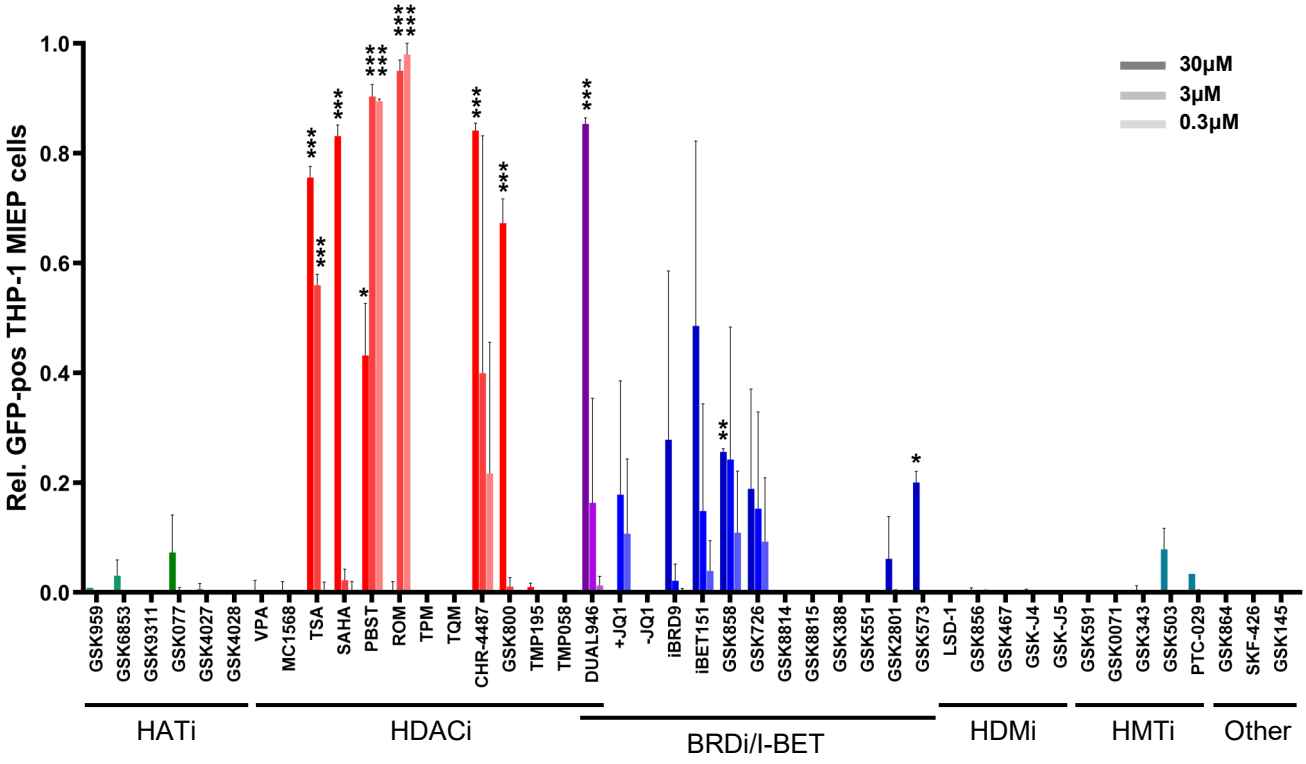

Figure S2. HDACis and I-BETs induce high level of MIEP activity in a monocytic cell model. THP-1 monocytes with an integrated MIEP driving GFP expression were treated with inhibitors of histone acetyltransferases (HATi, green), histone deacetylases (HDACi, red), bromodomain proteins (BRDi/I-BET, blue), histone demethylases (HDMi, orange), histone methyltransferases (HMTi, teal) as well as other epigenetic modifiers (Other, pink) across a range of concentrations (30-0.3μM) for 48 hours. GFP expression was then analysed by flow cytometry in comparison to DMSO (negative control) and PMA (100nM, positive control; set to 1). *n* = 3; bars = mean +SEM. **P*<0.05, ***P*<0.01, ****P*<0.001.

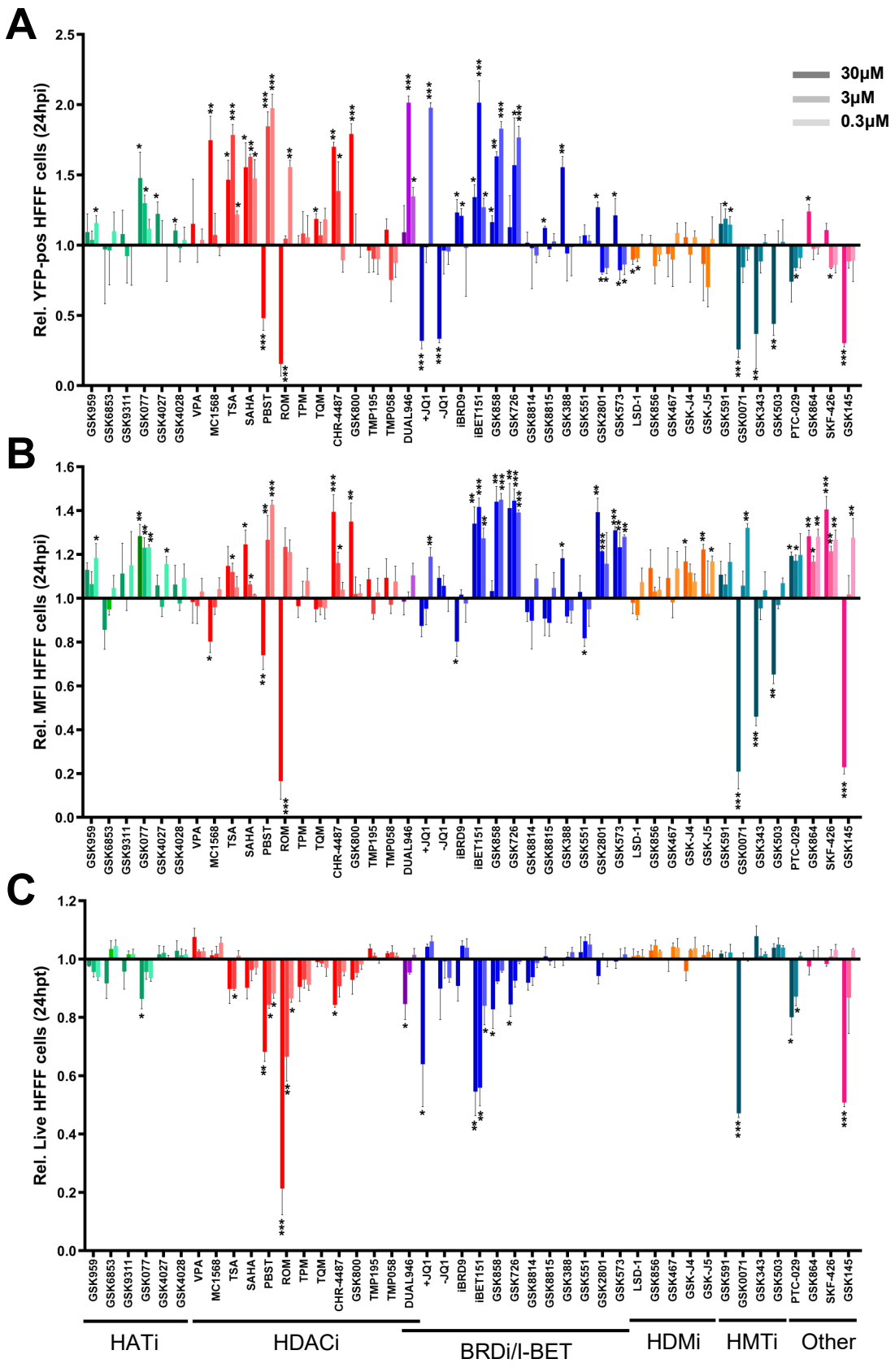

Figure S3. HDACis and I-BETs augment IE gene expression in HCMV lytically infected fibroblasts. Human foetal foreskin fibroblasts (HFFFs) were treated with inhibitors of histone acetyltransferases (HATi, green), histone deacetylases (HDACi, red), bromodomain proteins (BRDi/I-BET, blue), histone demethylases (HDMi, orange), histone methyltransferases (HMTi, teal) as well as other epigenetic modifiers (Other, pink) across a range of concentrations (30-0.3μM) for 16 hours before infection with HCMV TB40e IE86-eYFP (MOI 1). The number of YFP-positive cells (A) and level of YFP expression per cell (B) was then assessed at 24hpi, as well as the number of live cells by Hoechst stain (C) relative to DMSO (negative control; set to 1). *n* = 3; bars = mean +SEM. MFI, mean fluorescence intensity. **P*<0.05, ***P*<0.01, ****P*<0.001.

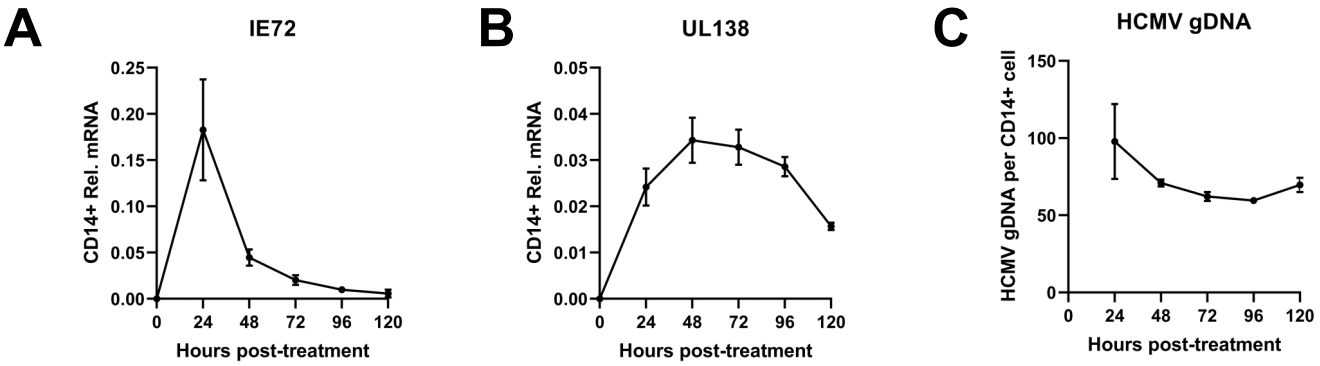

Figure S4. Experimental infection of CD14+ monocytes with HCMV TB40e IE86-eYFP results in virus latency. CD14+ monocytes isolated from apheresis cones were infected with HCMV TB40e IE86-eYFP with RNA and DNA isolated from cells every 24h for 5 days. RT-qPCR was then performed for virus (A) immediate early IE72 and (B) latent UL138 transcripts relative to host GAPDH and (C) HCMV genome copy number by UL44 promoter copy number relative to host GAPDH promoter. *n* = 3; points = mean ±SEM.

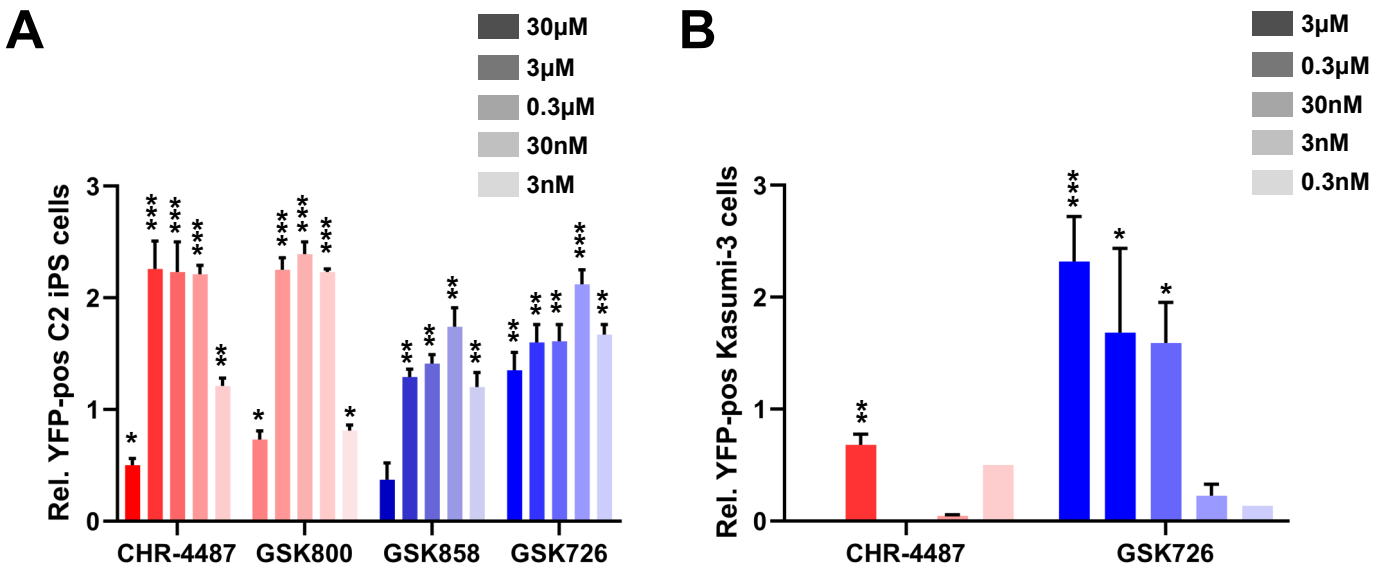

Figure S5. I-BETs induce IE gene expression from HCMV latently infected CD34+ cell models. (A) Human C2 induced pluripotent stem (iPS) cells and (B) Kasumi-3 CD34+ cells were both infected with HCMV TB40e IE86-eYFP for 3 days before treatment with HDACi (red bars) or I-BET (blue bars) across a range of concentrations (30μM to 0.3nM) for 48h. The number of YFP-positive cells was then counted per well in comparison to DMSO (negative control) and relative to PMA (100nM, positive control; set to 1). *n* = 3; bars = mean +SEM. **P*<0.05, ***P*<0.01, ****P*<0.001.

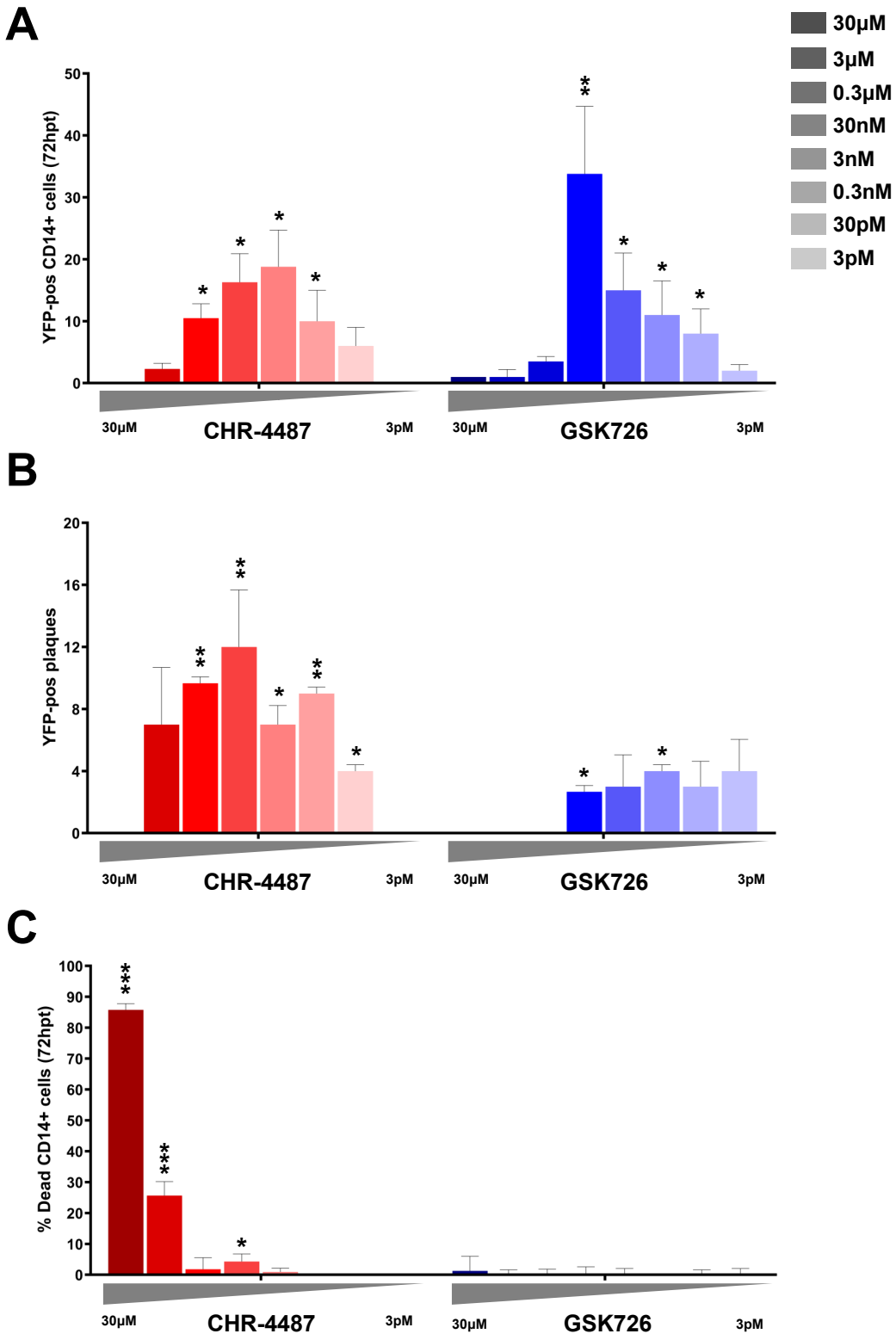

Figure S6. Further I-BET dilutions induce viral IE gene expression from HCMV latently infected CD14+ monocytes. (A) CD14+ monocytes isolated from apheresis cones were infected with HCMV TB40e IE86-eYFP for 5 days before treatment with HDACi (CHR-4487, red bars) or I-BET (GSK726, blue bars) across a range of concentrations (30μM to 3pM) for 72h. The number of YFP-positive cells per well was then counted, before (B) monocytes were overlaid with human foetal foreskin fibroblasts (HFFFs) and resulting plaques counted after 7 days. (C) CD14+ monocytes isolated from apheresis cones were treated with inhibitors for 72h before being stained with SYTOX (dead cells), Hoechst (nucleus) and counted. *n* = 3; bars = mean +SEM. **P*<0.05, ***P*<0.01, ****P*<0.001.

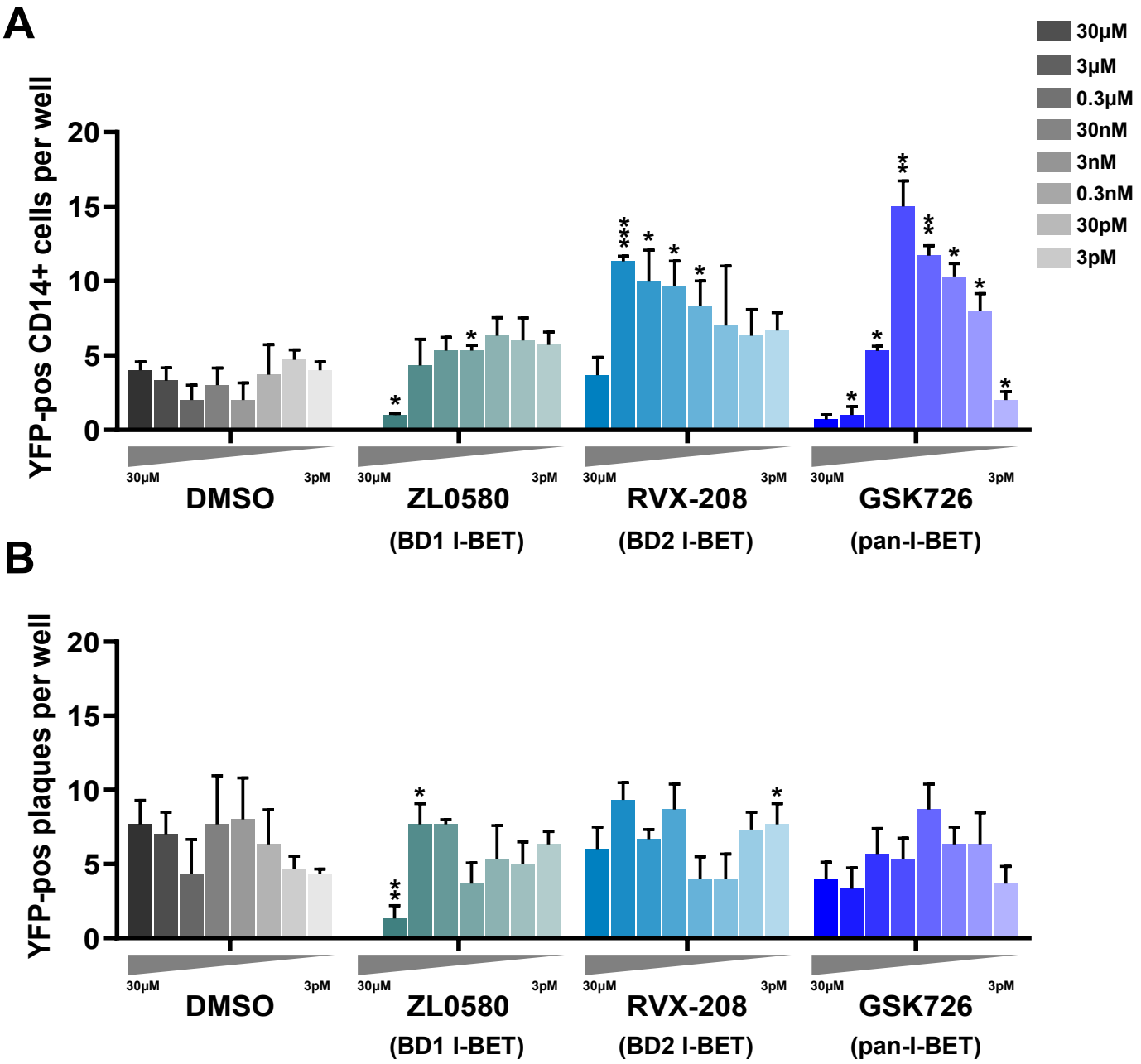

Figure S7. Bromodomain-2 (BD2)-selective I-BET, RVX-208, more closely phenocopies pan -I-BET, GSK726. (A) CD14+ monocytes isolated from apheresis cones were infected with HCMV TB40e IE86-eYFP for 5 days before treatment with DMSO, BD1-selective I-BET (ZL0580), BD2-selective I-BET (RVX-208) or pan-I-BET (GSK726) across a range of concentrations (30µM to 3pM) for 96h. The number of YFP-positive cells per well was then counted, before (B) monocytes were overlaid with human foetal foreskin fibroblasts (HFFFs) and resulting plaques counted after 7 days. (n = 3; bars = mean +SEM.) *P<0.05, **P<0.01, ***P<0.001.

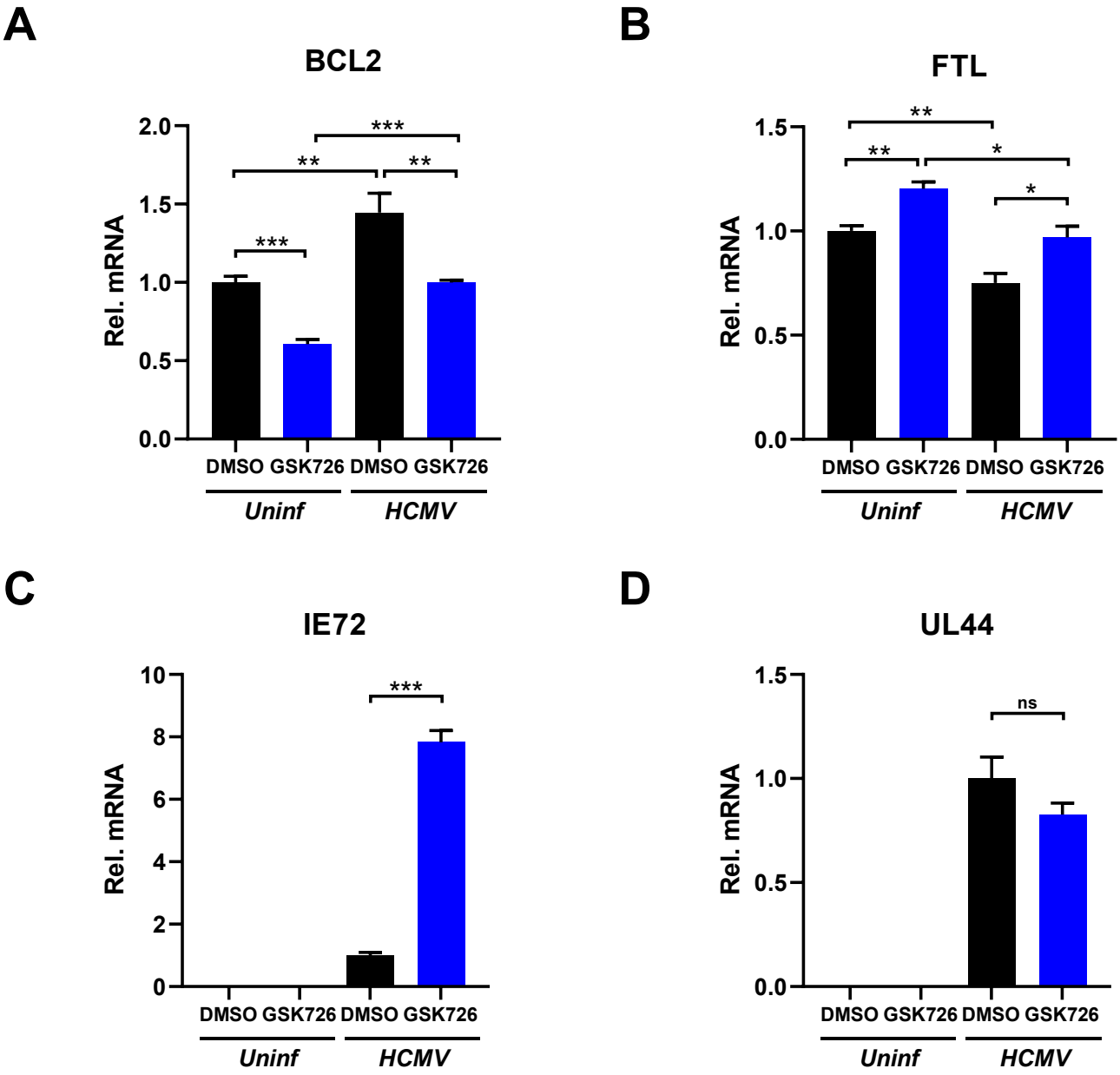

Figure S8. Modulation of CD14+ monocyte transcription with I-BET treatment. CD14+ monocytes isolated from apheresis cones remained uninfected (Uninf) or were infected (HCMV) with HCMV TB40e WT for 5 days before treatment with DMSO (black bars) or I-BET (GSK726 30nM, blue bars). RNA was isolated from cells after 24h and RT-qPCR then performed for BRD2/3/4 controlled cellular targets (A) BCL2 and (B) FTL or virus targets (C) IE72 and (D) UL44, all relative to host GAPDH (n = 3; data = mean +SEM). *P<0.05, **P<0.01, ***P<0.001, ns = not significant.

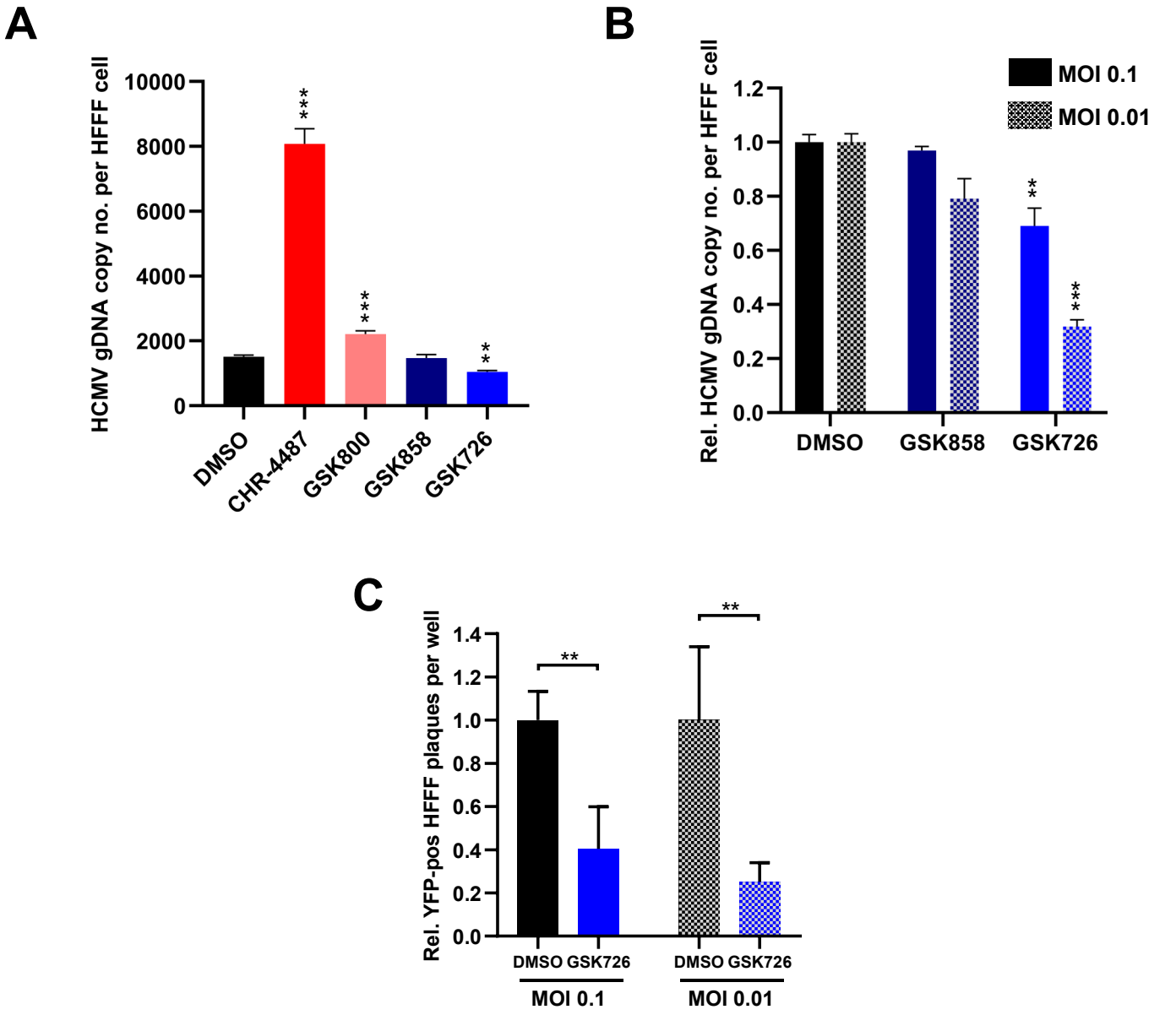

Figure S9. I-BETs restrict HCMV lytic DNA replication. (A) Human foetal foreskin fibroblasts (HFFFs) were treated with DMSO (control), HDACis (CHR-4487 and GSK800 at 30nM, red bars) and I-BETs (GSK858 and GSK726 at 30nM, blue bars) for 16 hours before infection with HCMV TB40e IE86-eYFP (MOI 0.1). After 72h, DNA was isolated and HCMV genome copy number determined per cell by qPCR of UL44 promoter relative to host GAPDH promoter (n = 3; bars = mean +SEM). (B) HCMV genome copy number data is shown relative to DMSO control (dark bars, data from Supplementary Fig. 7A) with the addition of further data from related experiments at MOI = 0.01 (hatched bars). (C) Tissue culture supernatants (96h post-infection) from comparable experiments to B were used to infect fresh HFFFs and subsequent YFP-pos plaques counted after 7 days relative DMSO controls. **P<0.01, ***P<0.001.

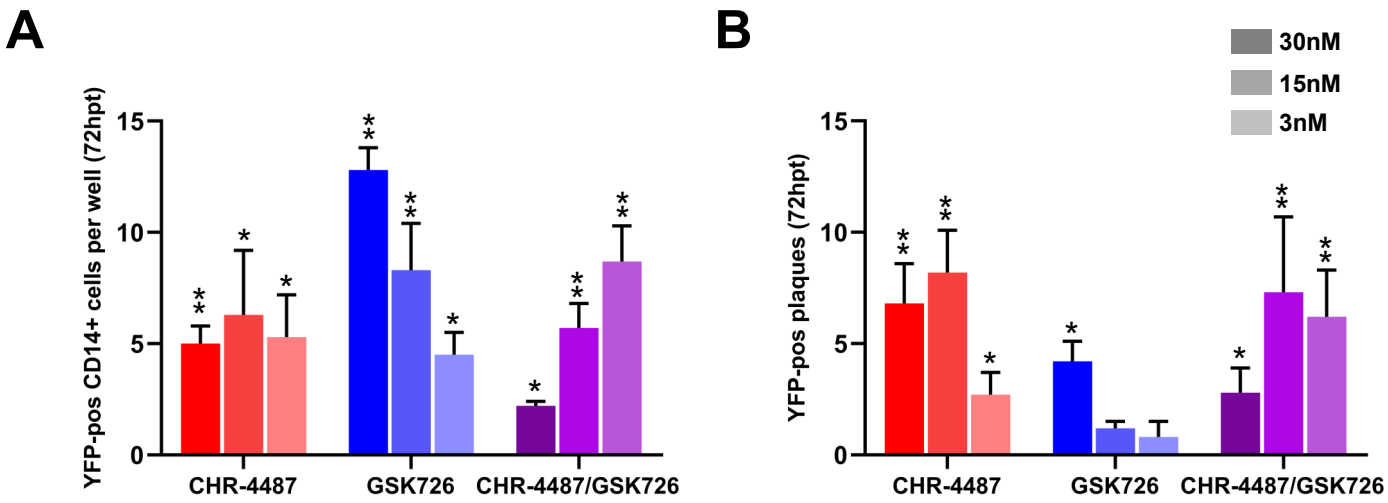

Figure S10. HDACi & I-BET co-treatment is additive at lower concentrations but does not restrict HCMV productive replication. (A) CD14+ monocytes isolated from apheresis cones were infected with HCMV TB40e IE86-eYFP for 5 days before treatment with HDACi (CHR-4487, red bars), I-BET (GSK726, blue bars) or co-treated with both (purple bars) across a range of concentrations (30nM to 3nM) for 72h. The number of YFP-positive cells per well was then counted, before (B) monocytes were overlaid with human foetal foreskin fibroblasts (HFFFs) and resulting plaques counted after 7 days. *n* = 3; bars = mean +SEM. **P*<0.05, ***P*<0.01.

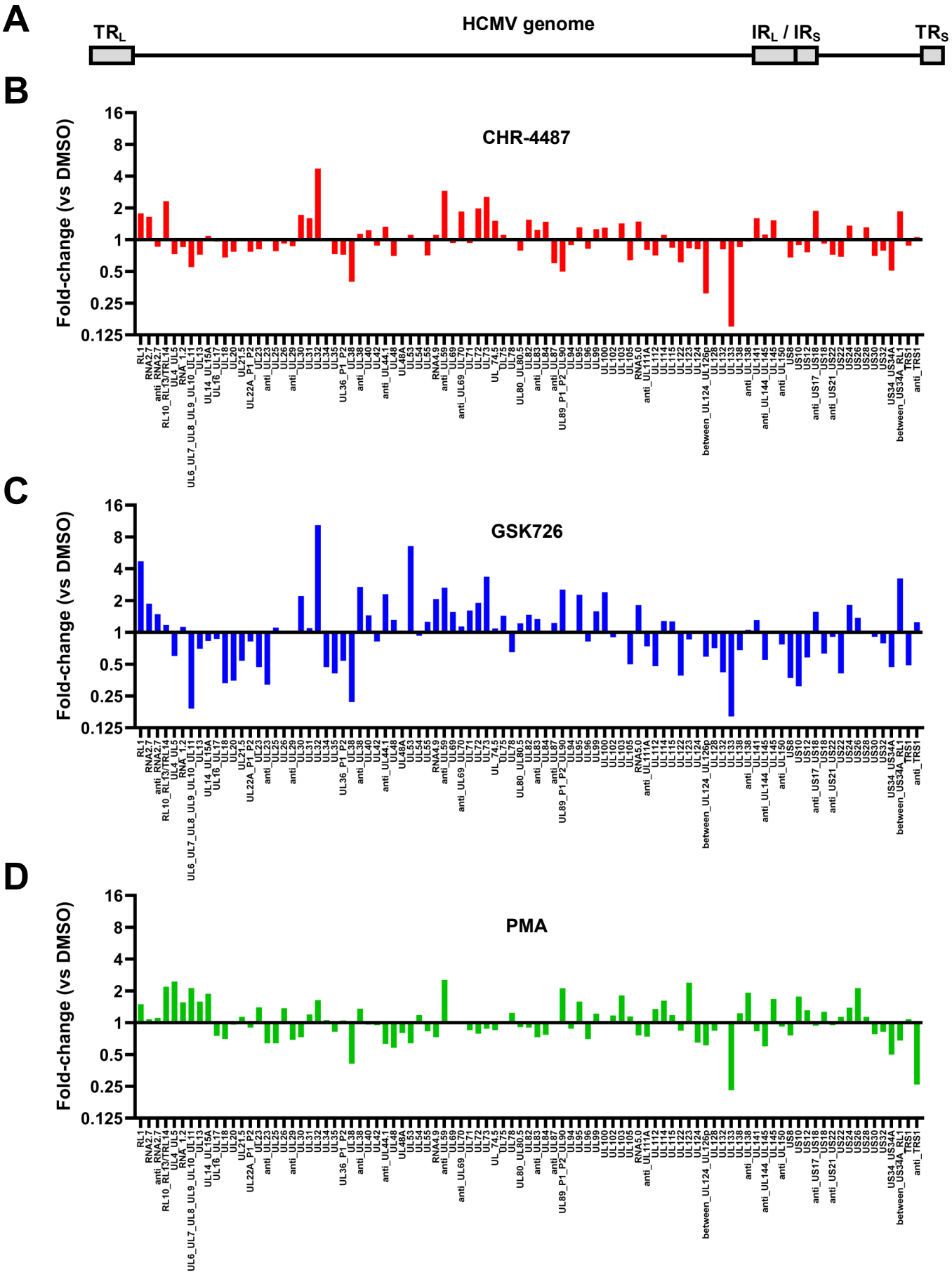

Figure S11. Modulation of HCMV latent transcript profiles with compound treatment. Schematic of linearised HCMV genome (A). Positionally aligned RNA-seq data from HCMV experimentally infected latent CD14+ monocytes treated with (B) HDACi (CHR-4487, red bars), (C) I-BET (GSK726, blue bars) or (D) PMA (green bars) relative to DMSO control (mean data from biological duplicates in Fig. 3F). IR_L = internal repeat long; IR_S = internal repeat short; TR_L = terminal repeat long; TR_S = terminal repeat short.

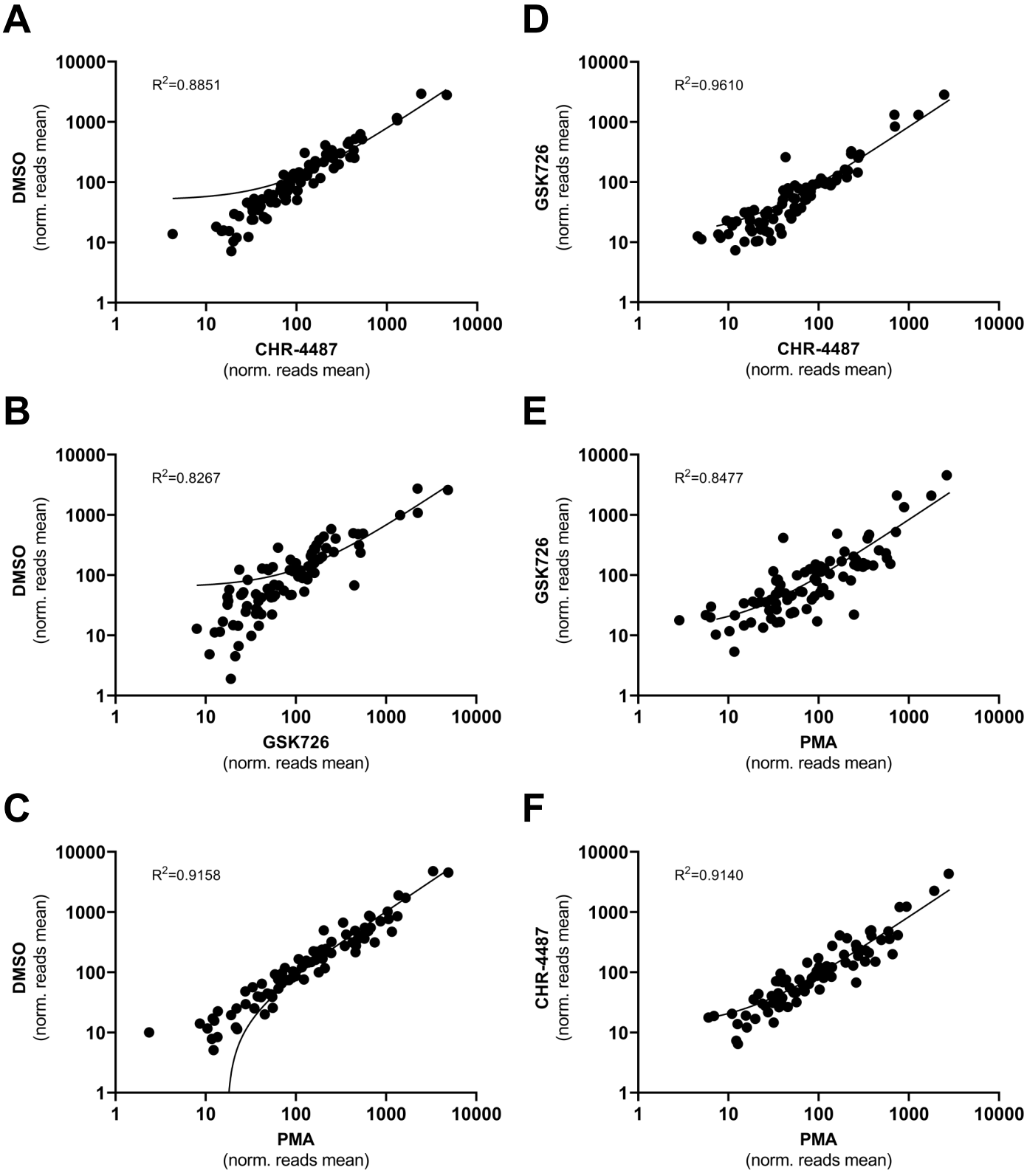

Figure S12. Relationships between HCMV latent transcript profiles with compound treatment. Correlations of HCMV transcript reads from RNA-seq data of HCMV experimentally infected latent CD14+ monocytes treated with DMSO, HDACi (CHR-4487), I-BET (GSK726) or PMA (mean data from biological duplicates in Fig. 3F).

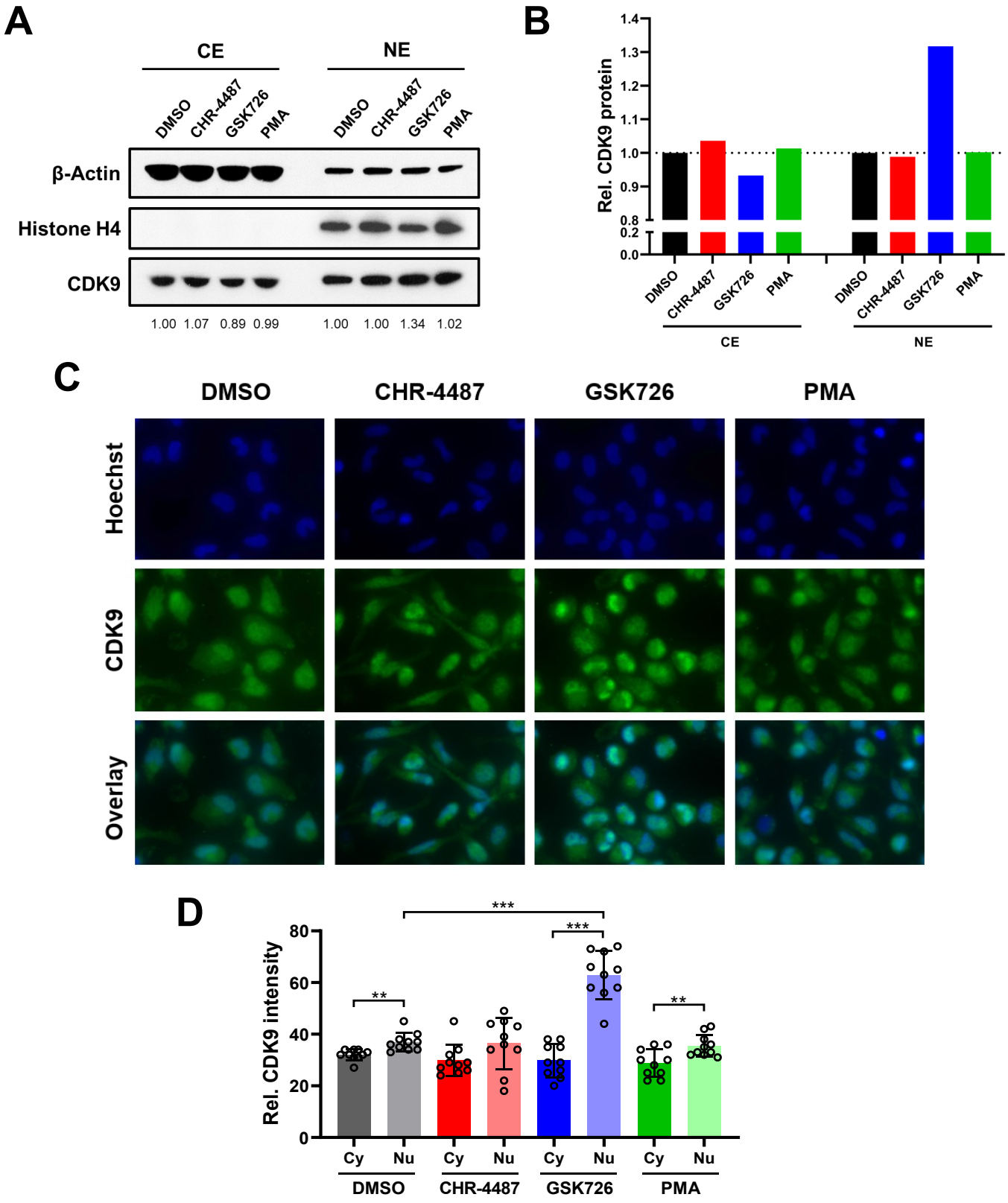

Figure S13. I-BETs cause release of CDK9 from cytosolic repressive complexes to the nucleus. CD14+ monocytes isolated from apheresis cones were treated with DMSO (black bars), HDACi (CHR-4487 30nM, red bars), I-BET (GSK726 30nM, blue bars) or PMA (20nM, green bars) for 24h before cells were lysed with nuclear (NE) and cytoplasmic (CE) protein fractions isolated by centrifugation. (A) Samples were then separated by SDS-PAGE and immunoblotted using specific antibodies for β-actin, histone H4 and CDK9 (representative of *n* = 2). (B) Resulting bands were then semi-quantified using ImageJ densitometry with CDK9 compared to the appropriate loading control (CE, β-actin; NE, histone H4) (mean of *n* = 2). (C, D) CD14+ monocytes treated as above for 24h were fixed and stained for CDK9 expression with Hoechst nuclear stain and the average intensity of cytoplasmic (Cy) and nuclear (Nu) expression quantified using Image J densitometry (***P*<0.01, ****P*<0.001).

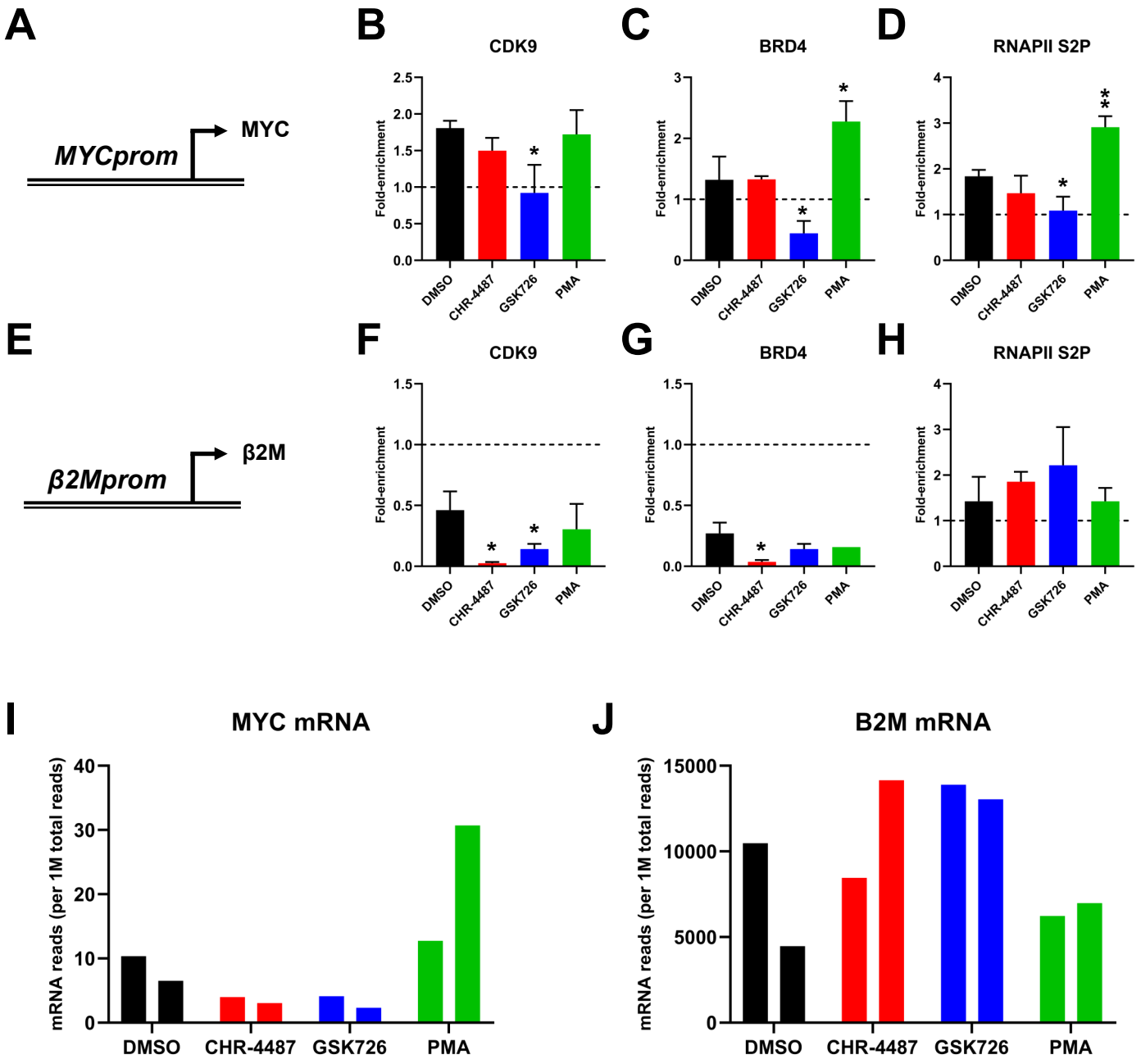

Figure S14. Chromatin immunoprecipitation (ChIP) host gene control data. Monocytic THP-1 cells were infected with HCMV TB40e IE86-eYFP for 3 days before treatment with DMSO (black bars), HDACi (CHR-4487 30nM, red bars), I-BET (GSK726 30nM, blue bars) or PMA (100nM, green bars). After 48h, cells were fixed and samples isolated for chromatin immunoprecipitation (ChIP) analysis. qPCR was then employed to determine the enrichment of (A-D) MYC- and (E-H) β2M-promoter DNA using antibodies specific for (B, F) CDK9, (C, G) BRD4, (D, H) RNAPII S2P relative to isotype controls (dotted line, set to 1) (n = 3; bars = mean +SEM). (I, J) RNA-seq data from isolated YFP-positive CD14+ monocytes infected with HCMV TB40e IE86-eYFP for 5 days before treatment with DMSO (black bars), HDACi (CHR-4487 30nM, red bars) or I-BET (GSK726 30nM, blue bars) or PMA (20nM, green bars). Data from biological duplicates. *P<0.05, **P<0.01.

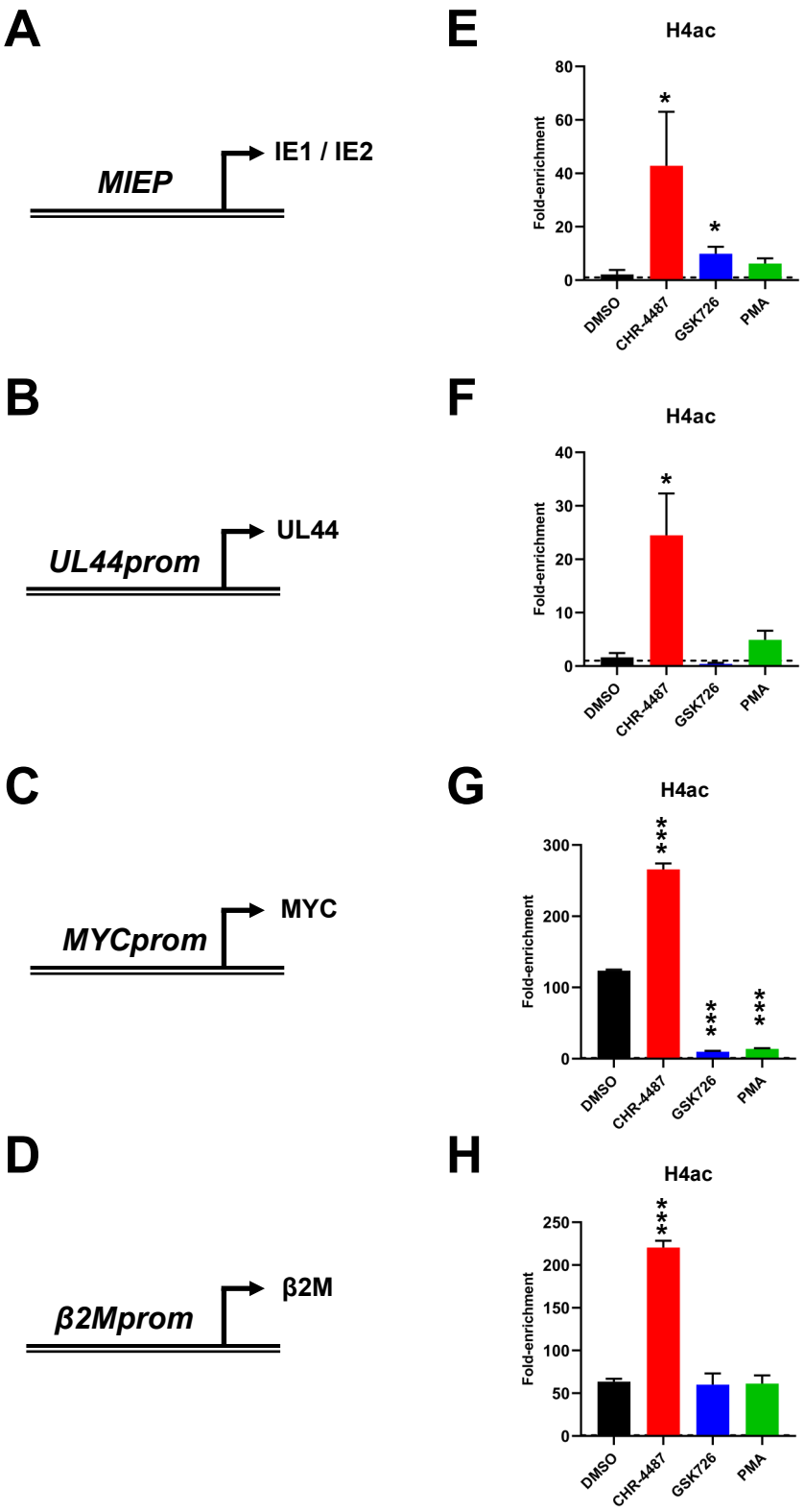

Figure S15. Histone acetylation is associated with promoter transcriptional activity and hyperacetylation with HDACi treatment. Monocytic THP-1 cells were infected with HCMV TB40e IE86-eYFP for 3 days before treatment with DMSO (black bars), HDACi (CHR-4487 30nM, red bars), I-BET (GSK726 30nM, blue bars) or PMA (100nM, green bars). After 48h, cells were fixed and samples isolated for chromatin immunoprecipitation (ChIP) analysis. qPCR was then employed to determine the enrichment of (A, B) MIEP, (C, D) UL44-, (E, F) MYC- and (G, H) β2M-promoter DNA using antibodies specific for (B, D, F, H) acetylated histone H4 (H4ac) relative to isotype control (dotted line, set to 1) (n = 3; bars = mean +SEM). *P<0.05, ***P<0.001.

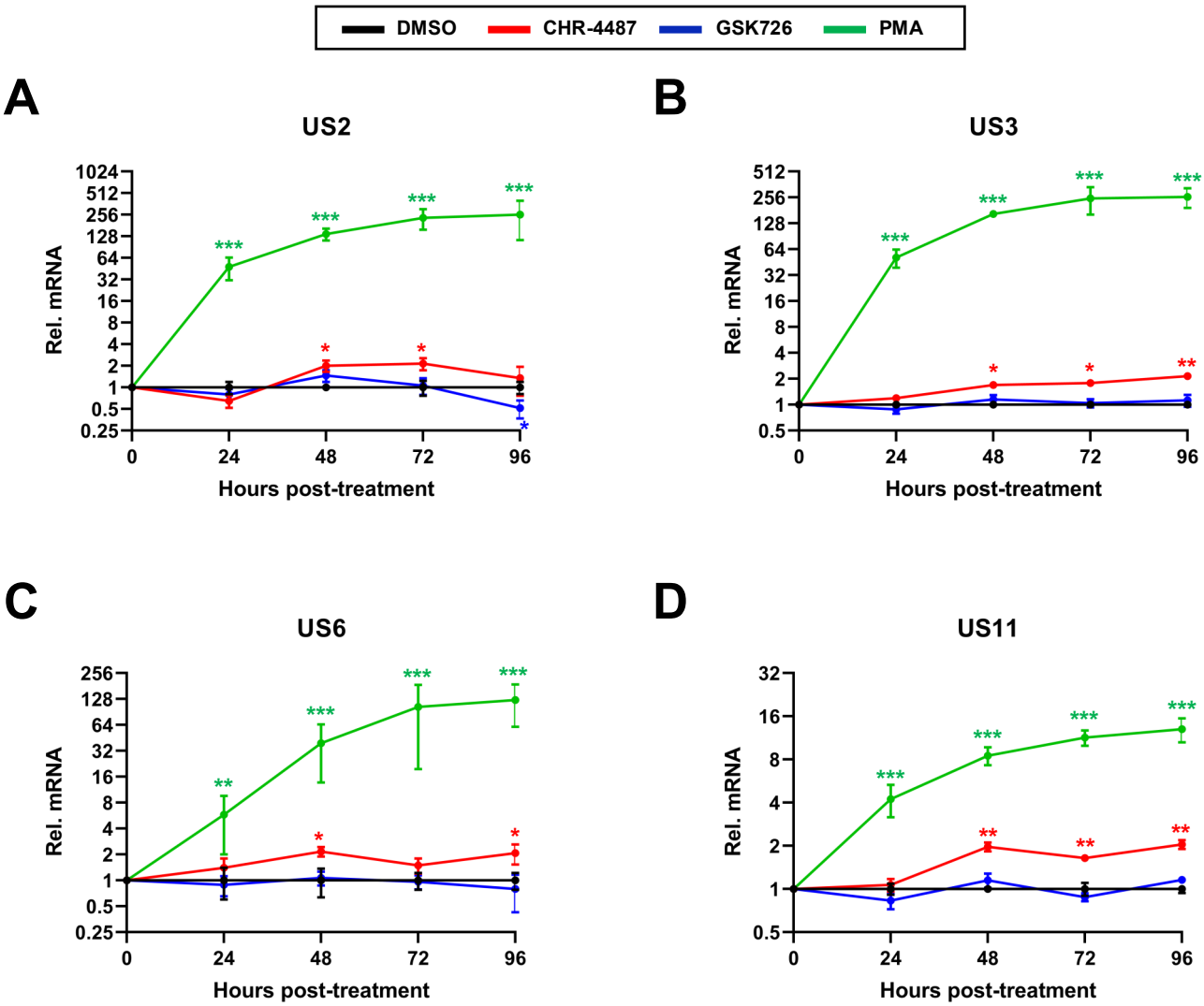

Figure S16. I-BET treatment does not lead to transcriptional increase of HCMV immune evasion genes US2, US3, US6 or US11. CD14+ monocytes isolated from apheresis cones were infected with HCMV TB40e WT for 5 days before treatment with DMSO (black lines), HDACi (CHR-4487 30nM, red lines), I-BET (GSK726 30nM, blue lines) and PMA (20nM, green lines). RNA was isolated from cells every 24h for 4 days and RT-qPCR was then performed for virus immune evasion genes (A) US2, (B) US3, (C) US6 and (D) US11 relative to host GAPDH (n = 3; data = mean ±SEM). *P<0.05, **P<0.01, ***P<0.001.

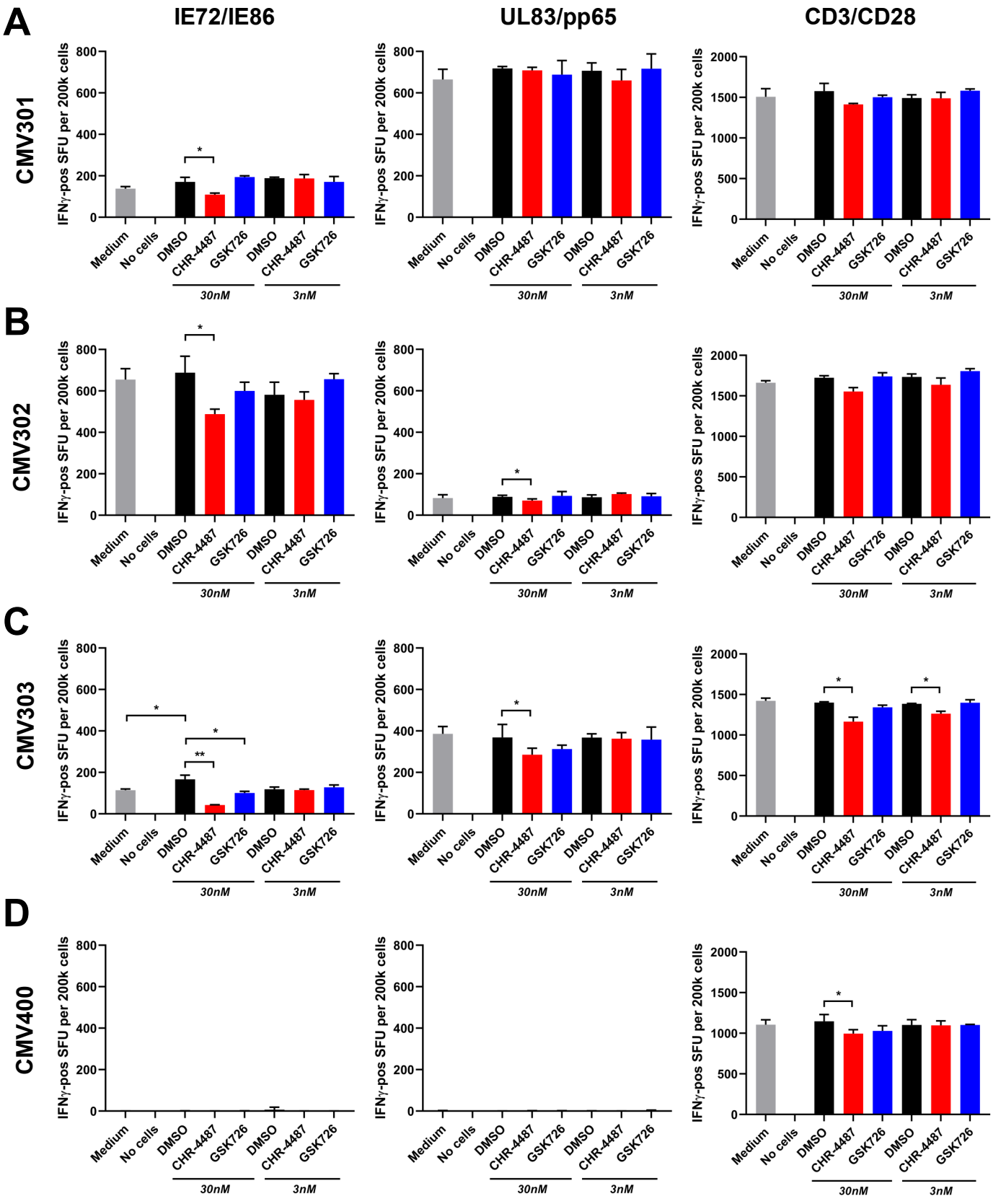

Figure S17. I-BETs do not inhibit T cell responses to HCMV-specific antigen stimulation. Peripheral blood was harvested from three seropositive donors (A-C) and one seronegative (D) donor before isolation of peripheral blood mononuclear cells (PBMC) by centrifugation. Fluorospot plates were then seeded with 200k PBMC and treated with DMSO (black bars), HDACi (CHR-4487, red bars) or I-BET (GSK726, blue bars) (30nM and 3nM) with concurrent treatment of HCMV-specific peptides for IE72/IE86 (left column), UL83/pp65 (middle column) or T cell activator CD3/CD28 (right column). After 48h, plates were processed and IFNγ-specific spot forming units (SFU) counted. *P*-values (Student's t-test): **P*<0.05, ***P*<0.01. (*n* = 3; data = mean +SEM).

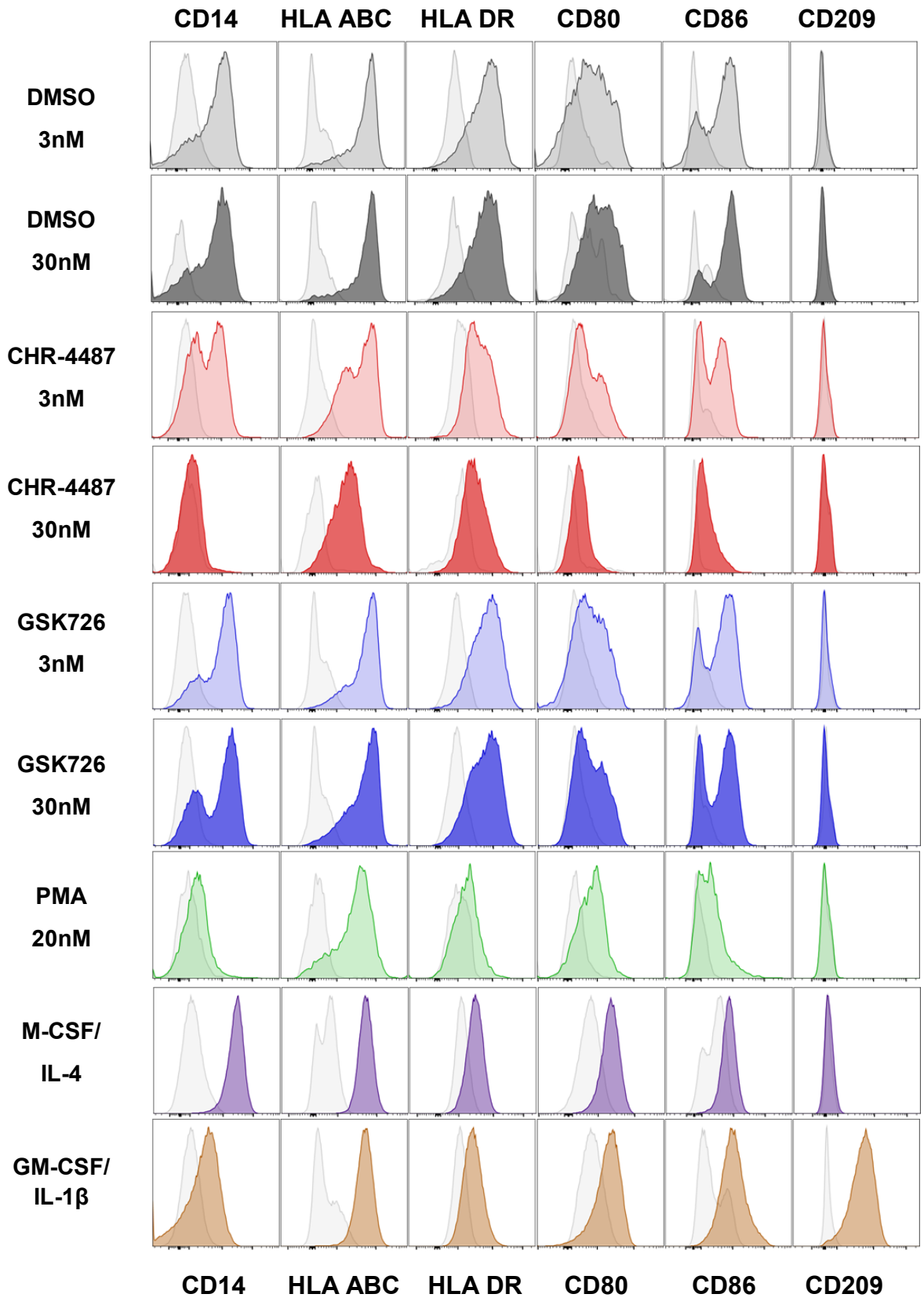

Figure S18. I-BETs do not differentiate CD14+ monocytes at concentrations that induce IE gene expression from latently infected CD14+ monocytes. CD14+ monocytes were isolated from apheresis cones and treated for 96h with compounds: DMSO (negative control, equivalent concentration); HDACi (CHR-4487, red peaks, 3nM/30nM); I-BET (GSK726, blue peaks, 3nM/30nM); PMA (positive control, green peaks, 20nM); M-CSF/IL-4 (macrophage differentiation, purple peaks); and GM-CSF/IL-1β (dendritic cell differentiation, orange peaks). Cells were then stained for differentiation markers: CD14 (monocyte); HLA ABC (MHC class I); HLA DR (MHC class II); CD80 (monocyte/macrophage); CD86 (monocyte/macrophage); CD209 (dendritic cell). Surface expression was then assessed by flow cytometry compared to isotype controls (light grey peaks throughout).

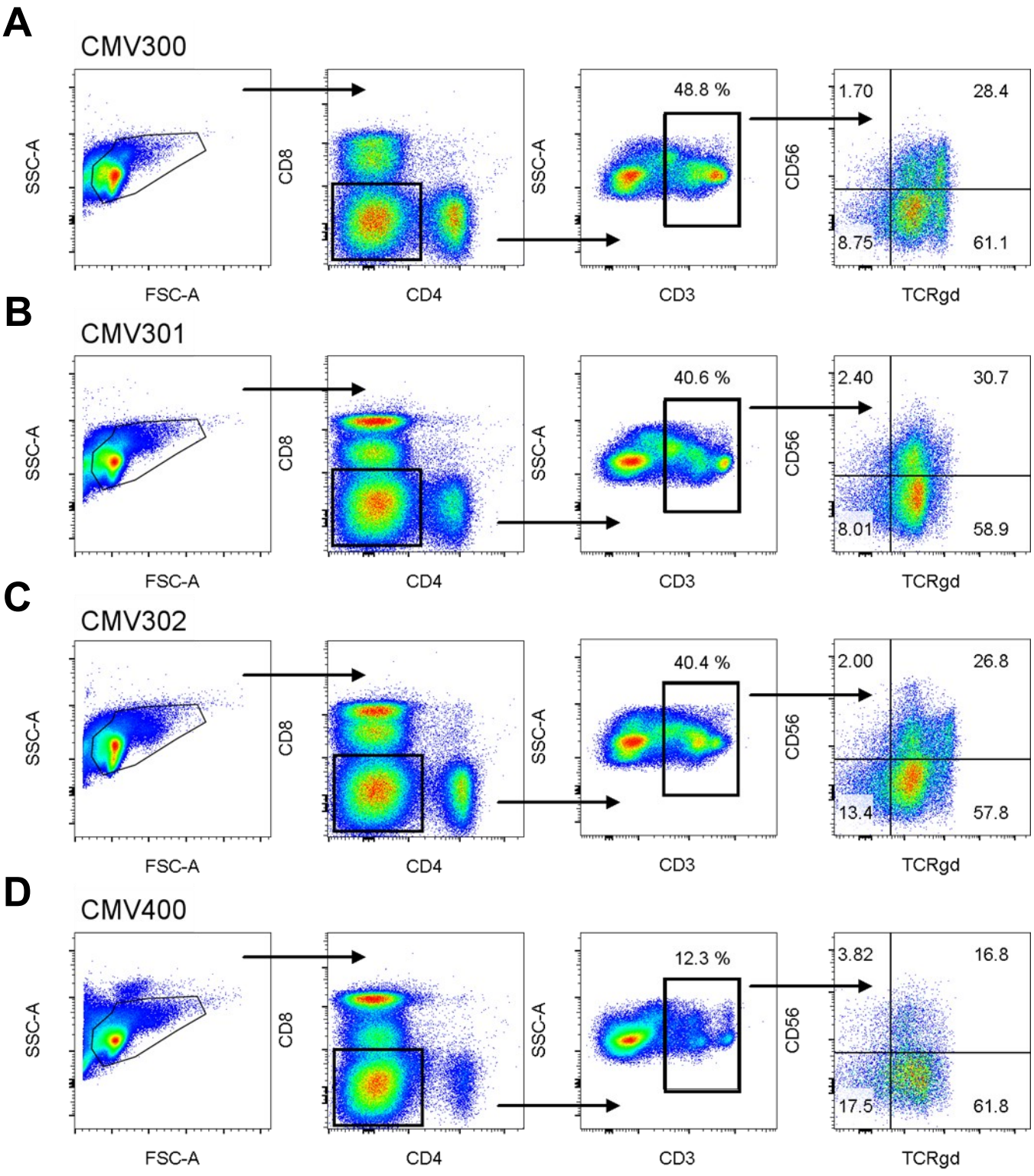

Figure S19. CD3+/CD4–/CD8– cytotoxic cells have γ/δ T cells markers. Total peripheral blood mononuclear cells (PBMC) were isolated from three seropositive donors (A-C) and one seronegative donor (D) and stained for lymphocyte surface markers CD3, CD4, CD8 and T cell receptor (TCR) subtypes α/β and γ/δ. Cell populations were then phenotyped by flow cytometry.

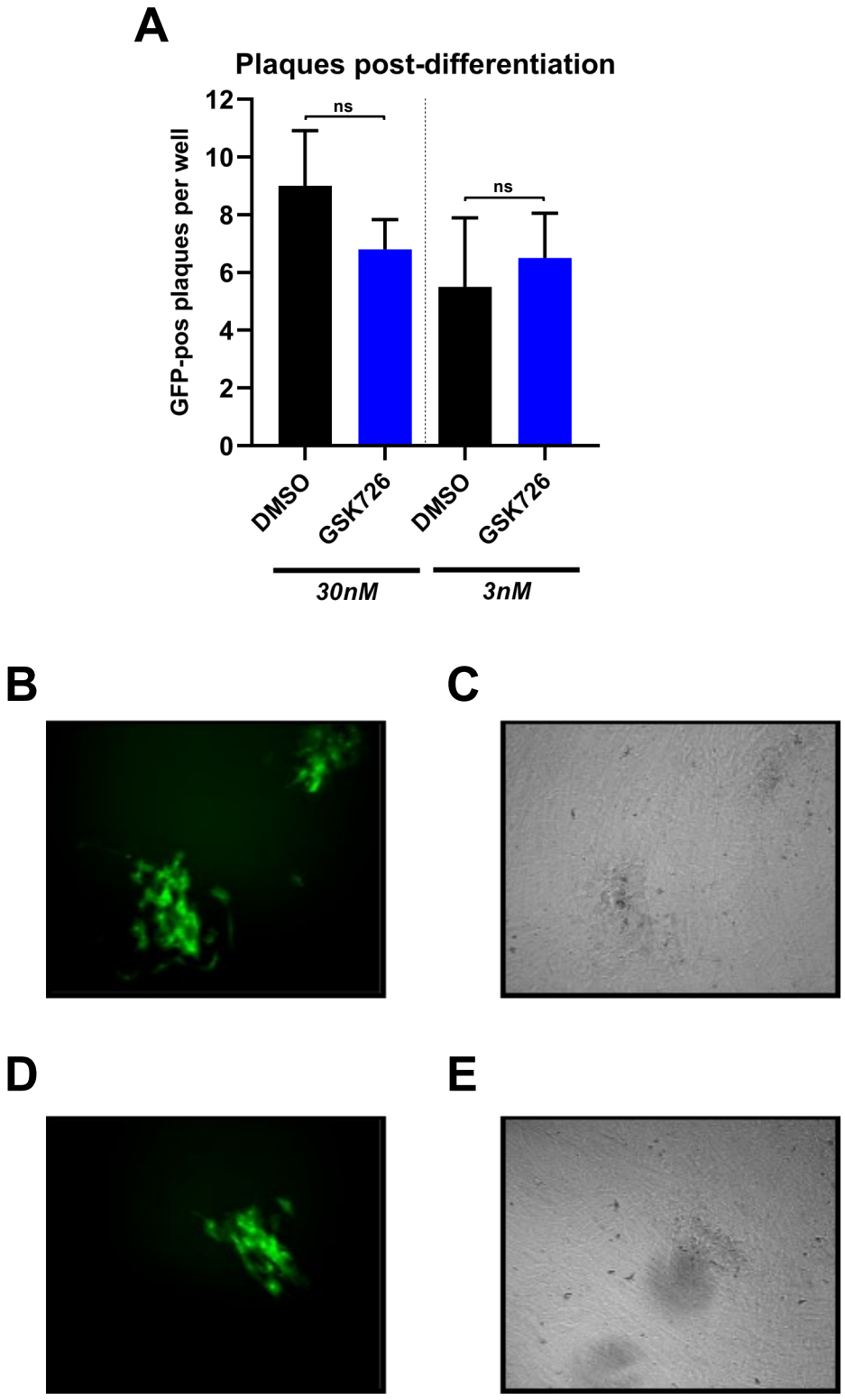

Figure S20. I-BET treatment does not inhibit HCMV DNA replication or productive infection after compound withdrawal and CD14+ monocyte differentiation. CD14+ monocytes isolated from apheresis cones were infected with HCMV TB40e UL32-GFP for 5 days before treatment with either DMSO (black bars) or I-BET (GSK726, blue bars) (30nM and 3nM) for 4 days. Treatments were then withdrawn and wells overlaid with human foetal foreskin fibroblasts (HFFFs) concurrent with CD14+ monocyte differentiation (M-CSF/IL-4) for 4 days. (A) Plaques were then counted (data = quadruplicate mean +SEM) with representative images shown for DMSO (B, GFP; C, brightfield) and GSK726 (D, GFP; E, brightfield) treatments. ns, not significant.

Supplementary Tables

Table S1. Epigenetic inhibitors and controls.

Compound	Full name	Target	Target activity	Source	Cat. no.
DMSO	Dimethyl sulphoxide	Control solvent	N/A	Sigma-Aldrich	D2650
GSK959		BRPF1	HAT	GlaxoSmithKline	
GSK6853		BRPF1	HAT	GlaxoSmithKline	
GSK9311		GSK6853 Neg Ctrl	(HAT)	GlaxoSmithKline	
GSK077		CBP/P300	HAT	GlaxoSmithKline	
GSK4027		PCAF/GCN5	HAT	GlaxoSmithKline	
GSK4028		GSK4027 Neg Ctrl	(HAT)	GlaxoSmithKline	
VPA	Valproic acid	HDAC Class I	HDAC	Cambridge Bioscience	13033
MC1568		HDAC Class IIa	HDAC	Cambridge Bioscience	16265
TSA	TrichostatinA	HDAC Class I, II & IV	HDAC	Sigma-Aldrich	T1952
SAHA	Vorinostat	HDAC Class I, II & IV	HDAC	Cambridge Bioscience	10009929
PBST	Panobinostat	HDAC Class I, II & IV	HDAC	Cambridge Bioscience	13280
ROM	Romidepsin	HDAC Class I	HDAC	Sigma-Aldrich	SML1175
TPM	Topirimate	HDAC	HDAC	Sigma-Aldrich	T0575
TQM	Tasquinimod	HDAC4	HDAC	Cambridge Bioscience	17692
CHR-4487		HDACi	HDAC	GlaxoSmithKline	
GSK800		CHR-4487 Neg Ctrl	(HDAC)	GlaxoSmithKline	
TMP195		Class Iia HDAC	HDAC	GlaxoSmithKline	
TMP058		TMP195 Neg Ctrl	(HDAC)	GlaxoSmithKline	
DUAL946		HDACi/BETi	HDAC/Bromo	GlaxoSmithKline	
+JQ1		pan-BET (BRD2/3/4/t)	Bromo	Sigma-Aldrich	SML1524
-JQ1		+JQ1 Neg Ctrl	(Bromo)	Sigma-Aldrich	SML1525
iBRD9		BRD9	Bromo	GlaxoSmithKline	
iBET151		pan-BET (BRD2/3/4/t)	Bromo	GlaxoSmithKline	
GSK858		pan-BET (BRD2/3/4/t)	Bromo	GlaxoSmithKline	
GSK726		pan-BET (BRD2/3/4/t)	Bromo	GlaxoSmithKline	
GSK8814		ATAD2/2B bromodomain	Bromo	GlaxoSmithKline	
GSK8815		GSK8814 Neg Ctrl	(Bromo)	GlaxoSmithKline	
GSK388		ATAD2 bromodomain	Bromo	GlaxoSmithKline	
GSK551		GSK388 Neg Ctrl	(Bromo)	GlaxoSmithKline	
GSK2801		BAZ2A/B	Bromo	GlaxoSmithKline	
GSK573		BAZ2A/B, GSK2801 Neg Ctrl	(Bromo)	GlaxoSmithKline	
LSD-1		LSD1	HDM	GlaxoSmithKline	
GSK856		Jarid1a/b/c	HDM	GlaxoSmithKline	
GSK467		KDM5/JARID1	HDM	GlaxoSmithKline	
GSK-J4		KDM6A/B & KDM5s	HDM	GlaxoSmithKline	
GSK-J5		GSK-J4 Neg Ctrl	(HDM)	GlaxoSmithKline	
GSK591		PRMT5	HMT	GlaxoSmithKline	
GSK0071		G9a/GLP	HMT	GlaxoSmithKline	
GSK343		EZH2	HMT/PRC2	GlaxoSmithKline	
GSK503		EZH2	HMT/PRC2	GlaxoSmithKline	
PTC-029		Bmi-1i / PRC1i	PRC1	Sigma-Aldrich	SML1143
GSK864		mutant IDH1	Other	GlaxoSmithKline	
SKF-426		Checkpoint inhibitor	Other	GlaxoSmithKline	
GSK145		HIV reactivation	Other	GlaxoSmithKline	
FLAV	Flavopiridol	CDK9	CDK9i	Sigma-Aldrich	F3055
dBET1		BRD4	BRD4 protac	Cambridge Bioscience	CAY18044
RVX-208	Apabetalone	BRD4 bromodomain 2	Bromo	Cambridge Bioscience	CAY16424
ZL1580		BRD4 bromodomain 1	Bromo	Cambridge Bioscience	HY-126428
KL-2		SEC	SECi	Sigma Aldrich	SML2538

(Bromo, bromodomain; CDK9, cyclin dependent kinase 9; HAT, histone acetyltransferase; HDAC, histone acetyltransferase; HDM, histone demethylase; HMT, histone methyltransferase; N/A, not applicable; PRC, polycomb repressive complex; SEC, super-elongation complex.)

Table S2. HCMV latently infected CD14+ monocyte RNA-seq data: HCMV transcript fold-change levels.

	Mean fold-change vs DMSO			From: (13)	From: (14)
HCMV gene*	**CHR-4487**	**GSK726**	**PMA**	**Protein function**	**Temporal expression profile (Tp)**
UL32	4.72	10.37	1.64	tegument protein pp150	Tp5
UL53	1.11	6.56	0.64	nuclear egress lamina protein	Tp5
RL1	1.78	4.73	1.50	unknown	Tp3
UL73	2.55	3.36	0.88	envelope glycoprotein N	Tp5
between_US34A_RL1	1.86	3.24	0.68	RNA	N/A
anti_UL38	1.14	2.70	1.36	antisense RNA	N/A
anti_UL59	2.91	2.65	2.55	antisense RNA	N/A
UL89_P1_P2_UL90	0.50	2.55	2.12	terminase ATPase subunit	Tp5
UL100	1.30	2.41	1.03	envelope glycoprotein M	Tp5
anti_UL44.1	1.33	2.30	0.63	antisense RNA	N/A
UL95	1.31	2.27	1.59	tegument protein	Tp3
UL30	1.72	2.21	0.73	latency?	Tp5
RNA4.9	1.11	2.07	0.73	lncRNA	N/A
UL72	1.98	1.90	0.79	tegument protein	Tp3
RNA2.7	1.65	1.87	1.08	lncRNA	N/A
US24	1.36	1.82	1.39	tegument protein	Tp1
RNA5.0	1.49	1.81	0.76	lncRNA	N/A
UL71	0.93	1.61	0.85	tegument protein	Tp3
UL99	1.26	1.59	1.22	myristylated tegument protein pp28	Tp5
anti_US17_US18	1.88	1.57	0.94	antisense RNA	N/A
UL69	0.93	1.56	1.00	deoxyuridine triphosphatase	Tp3
anti_RNA2.7	0.86	1.49	1.11	antisense RNA	N/A
UL82	1.55	1.47	0.90	tegument protein pp71	Tp5
UL40	1.23	1.45	0.96	membrane glycoprotein	Tp3
UL75	1.11	1.44	1.02	envelope glycoprotein H	Tp5
US26	0.97	1.38	2.13	unknown	Tp3
anti_UL83	1.24	1.34	0.73	antisense RNA	N/A
UL48	0.70	1.32	0.58	large tegument protein	Tp5
UL141	1.60	1.31	0.83	membrane glycoprotein	Tp5
UL114	1.11	1.28	1.62	uracil-DNA glycosylase	Tp2
UL115	0.84	1.27	1.18	envelope glycoprotein L	Tp5
UL55	0.71	1.26	0.83	envelope glycoprotein B	Tp5
anti_TRS1	1.06	1.25	0.26	antisense RNA	N/A
anti_UL87	0.60	1.23	1.03	antisense RNA	N/A
UL80_UL80.5	0.79	1.22	0.91	capsid maturation protease	Tp3
RL10_RL13/TRL14	2.32	1.18	2.19	glycoprotein	Tp5
anti_UL69_UL70	1.85	1.14	0.99	antisense RNA	N/A
RNA_1.2	0.85	1.13	1.56	lncRNA	N/A
UL25	0.78	1.11	0.64	tegument protein	Tp5
UL31	1.60	1.10	1.20	phosphoprotein	Tp5
UL_74.5	1.51	1.09	0.85	unknown	Tp5
anti_UL138	0.96	1.06	1.93	antisense RNA	N/A
UL124	0.81	1.04	0.65	membrane glycoprotein	Tp3
UL48A	1.03	1.02	0.80	small capsid protein	Tp5
UL145	1.53	1.01	1.68	degradation protein	Tp3
UL84	1.48	0.99	0.77	DNA replication protein	Tp5
anti_UL29	0.87	0.99	0.69	antisense RNA	N/A
UL94	0.89	0.99	0.88	tegument protein	Tp5
US28	1.43	0.98	1.81	membrane protein / GPCR / transcription regulator / latency associated	Tp4
UL103	1.31	0.98	1.14	tegument protein	Tp3
UL26	0.92	0.97	1.37	tegument protein	Tp5
UL54	1.01	0.93	1.18	DNA polymerase catalytic subunit	Tp2
US30	0.72	0.91	0.95	membrane protein	Tp4

anti_US21_US22	0.70	0.91	0.78	antisense RNA	N/A
UL102	0.97	0.90	1.17	DNA helicase-primase subunit	Tp3
UL16_UL17	0.96	0.87	0.75	immunomodulation	Tp2_Tp4
UL123	0.83	0.86	2.40	regulatory protein IE1 / IE72	Tp1
UL96	1.09	0.83	1.88	tegument protein	ND
UL14_UL15A	0.88	0.82	0.95	membrane protein/glycoprotein	Tp2_Tp3
UL22A_P1_P2	0.82	0.82	0.70	secreted glycoprotein	Tp5
UL42	0.77	0.82	0.90	putative membrane protein	ND
US32	0.79	0.79	0.82	unknown	ND
anti_UL150	1.01	0.77	0.92	antisense RNA	N/A
anti_UL111A	0.80	0.74	0.74	antisense RNA	N/A
UL128	1.01	0.71	0.84	putative secreted protein / envelope protein	ND
UL13	0.72	0.70	1.59	putative secreted protein	Tp1
UL138	0.85	0.68	1.23	latency-associated protein	Tp1
UL78	1.01	0.65	1.24	immunomodulation / GPCR	Tp2
US18	0.92	0.63	1.27	putative multiple transmembrane protein	ND
UL4_UL5	0.73	0.60	2.46	glycoprotein	Tp5
between_UL124_UL126p	0.31	0.59	0.61	RNA	N/A
US12	0.76	0.58	1.31	utative multiple transmembrane protein	Tp2
anti_UL144_UL145	1.12	0.55	0.60	antisense RNA	N/A
UL21.5	1.02	0.54	1.14	immunomodulation / DNA synthesis / cell cycle modulation	ND
UL36_P1_P2	0.72	0.54	1.05	tegument protein vICA / apoptosis / DNA replication	Tp2
UL105	0.64	0.50	1.15	helicase-primase helicase subunit / DNA replication	Tp3
TRS1	0.88	0.49	1.08	tegument protein / DNA replication	Tp4
UL112	0.71	0.48	1.35	DNA replication / transcription activator	Tp5
UL23	0.99	0.47	1.06	tegument protein	Tp3
US34_US34A	0.81	0.47	1.40	membrane / sectreted protein	ND
UL34	0.51	0.47	0.50	transcription activator	Tp3
UL132	0.81	0.42	1.02	envelope glycoprotein	Tp5
UL35	0.73	0.41	0.82	tegument protein	Tp5
US22	0.69	0.41	1.14	tegument protein	Tp3
UL122	0.61	0.39	0.84	regulatory protein IE2 / IE86	Tp1
US8	0.68	0.37	0.76	membrane glycoprotein / immunomodulation	Tp3
UL20	0.77	0.35	0.96	transmembrane protein	ND
UL18	0.68	0.33	0.70	membrane glycoprotein / immunomodulation	ND
anti_UL23	1.03	0.32	0.64	antisense RNA	N/A
US10	0.89	0.31	1.77	membrane glycoprotein / immunomodulation	Tp2
UL38	0.40	0.22	0.41	glycoprotein	Tp2
UL6_UL7_UL8_UL9_UL10_UL11	0.55	0.19	2.13	various / immunomodulation	Various
UL133	0.15	0.16	0.23	putative membrane protein / latency	Tp2

(ND = not determined; N/A = not applicable.)

HCMV gene - *asterisk colours as per heatmap in Fig. 3F:

Structural protein
Long non-coding RNA
Immunomodulatory protein
DNA replication protein

Table S3. Primers and conditions of use for qPCR.

Oligo name	Oligo sequence (5' to 3')	Protocol	Design Reference
GAPDH sense	TGCACCACCAACTGCTTAGC	RT-qPCR	15
GAPDH antisense	GGCATGGACTGTGGTCATGAG		
IE72 sense	GTCCTGACAGAACTCGTCAAA	RT-qPCR	16
IEexon4 antisense	TAAAGGCGCCAGTGAATTTTTCTTC		
UL44 sense	TACAACAGCGTGTCGTGCTCCG	RT-qPCR	17
UL44 antisense	GGCGTAAAAAACATGCGTATCAAC		
UL83/pp65 sense	GGGACACAACACCGTAAAGCCG	RT-qPCR	17
UL83/pp65 antisense	CGTGGAAGAGGACCTGACGATGAC		
UL138 sense	ACGACGAAGACGATGAACCC	RT-qPCR	In house
UL138 antisense	CCCGATGAGATCTTGGTCCG		
US2 sense	AGCACACGAAAAACCGCATC	RT-qPCR	16
US2 antisense	TGCGGAAGTCATACACGCAT		
US3 sense	ACCGTGGATATGGTGGACAT	RT-qPCR	18
US3 antisense	AACAGCAGACCCCAATTGTC		
US6 sense	ATCTGCATCTGTGCAGTCCC	RT-qPCR	16
US6 antisense	TTCTCTCTCTGTCTCCGCGA		
US11 sense	TACTCCGAAACATCGGGCAG	RT-qPCR	16
US11 antisense	CGCGGGTAGTATGCCTGAAT		
BCL2 sense	AGTACCTGAACCGGCACCT	RT-qPCR	19
BCL2 antisense	CAGCCAGGAGAAATCAAACAG		
FTL sense	CAGCCTGGTCAATTTGTACCT	RT-qPCR	19
FTL antisense	GCCAATTCGCGGAAGAAGTG		
β2Mprom sense	CGGGCTCTGCTTCCCTTAGACT	ChIP-qPCR	19
β2Mprom antisense	TGCTAGGACATGCGAACTTAGC		
GAPDHprom sense	CGGCTACTAGCGGTTTTACG	ChIP-qPCR & gDNA quantification	20
GAPDHprom antisense	AAGAAGATGCGGCTGACTGT		
gB sense	GAGGACAACGAAATCCTGTTGGGCA	Natural HCMV gDNA quantification	21
gB antisense	GTCGACGGTGGAGATACTGCTGAGG		
MIEP sense	CCAAGTCTCCACCCCATTGAC	ChIP-qPCR	22
MIEP antisense	GACATTTTGGAAAGTCCCGTTG		
MYCprom sense	GAGCAGCAGAGAAAGGGAGA	ChIP-qPCR	19
MYCprom antisense	CAGCCGAGCACTCTAGCTCT		
UL44prom sense	AACCTGAGCGTGTTTGTG	Experimental HCMV gDNA quantification	23
UL44prom antisense	CGTGCAAGTCTCGACTAAG		

Conditions used: 95°C for 60sec; 40 cycles of 95°C for 15sec, 60°C for 30sec (read); followed by melt curve analysis from 60°C to 95°C to confirm product specific amplification.

Table S4. Antibodies and conditions of use for chromatin immunoprecipitation, immunofluorescence, immunoblot analysis and cell phenotyping.

Target	Supplier	Cat. No.	Protocol	Clone	Isotype	Fluorophore	Volume/Mass/Dilution
H4ac	Active Motif	39925	ChIP				5 µg
IgG Rabbit	Abcam	ab171870	ChIP				Variable
IgG Rat	Diagenode	C15420001	ChIP				Variable
CDK9	Abcam	ab239364	IB				0.6 mg/ml
			ChIP				5 µg
			IF				6 µg/ml
BRD4	Active Motif	39909	ChIP				4.2 µg
			IB				1:1,000
Histone H4(pan)	Bio-Rad	AHP413	IB				1:1,000
RNAPII Ser2P	Active Motif	61083	ChIP				10 µg
β-Actin	Abcam	ab8227	IB				1 mg/ml
IE72/IE1	Argene	11-003	IB				1:500
UL44	Virusys	10D8	IB				1:5,000
pp65/UL83	Santa Cruz	sc-56976	IB				0.1 µg/ml
Anti-Rabbit IgG 488	Abcam	ab150077	IF				2 µg/ml
Anti-Rabbit IgG HRP	Santa Cruz	sc-2357	IB				0.2 µg/ml
Anti-Mouse IgG HRP	Cell Signalling Technology	7076	IB				1:2,000
Normal mouse serum	Invitrogen	01-6501	FC				1:50
TruStain FcX	Biolegend	422302	FC				5 µl
TruStain Monocyte Blocker	Biolegend	426103	FC				5 µl
Live Dead stain	Thermofisher	L34966	FC			Aqua	2.5 µl
HLA DR	Biolegend	307636	FC	L243	IgG2aκ	BV421	2 µl
CD14	Biolegend	301824	FC	M5E2	IgG2aκ	PerCP-Cy5.5	3 µl
CD80	Biolegend	305210	FC	2D10	IgG1κ	PE-Cy5	4 µl
CD86	Biolegend	305422	FC	IT2.2	IgG2bκ	PE-Cy7	3 µl
CD209	Biolegend	330108	FC	9E9A8	IgG2aκ	APC	3 µl
HLA ABC	Biolegend	311438	FC	W6/32	IgG2aκ	AF700	3 µl
IgG2aκ-BV421 isotype control	Biolegend	400260	FC	MOPC-173	IgG2aκ	BV421	2 µl
IgG2aκ-PerCP-Cy5.5 isotype control	Biolegend	400251	FC	MOPC-173	IgG2aκ	PerCP-Cy5.5	3 µl
IgG1κ-PE-Cy5 isotype control	Biolegend	400118	FC	MOPC-21	IgG1κ	PE-Cy5	4 µl
IgG2bκ-PE-Cy7 isotype control	Biolegend	400326	FC	MPC-11	IgG2bκ	PE-Cy7	3 µl
IgG2aκ-APC isotype control	Biolegend	400222	FC	MOPC-173	IgG2aκ	APC	3 µl
IgG2aκ-AF700 isotype control	Biolegend	400248	FC	MOPC-173	IgG2aκ	AF700	3 µl
CD56	Biolegend	318327	FC	HCD56	IgG1κ	BV421	3 µl
CD4	Biolegend	317438	FC	OKT4	IgG1κ	BV605	2.5 µl
CD3	Biolegend	300406	FC	UCHT1	IgG1κ	FITC	2 µl
CD8	Biolegend	301032	FC	RPA-T8	IgG1κ	PerCP-Cy5.5	2 µl
TCR gamma delta	Biolegend	331209	FC	B1	IgG1κ	PE	3 µl
TCR alpha beta	Biolegend	306717	FC	IP26	IgG1κ	APC	3 µl

(ChIP = chromatin immunoprecipitation; IB = immunoblot; IF = immunofluorescence; FC = flow cytometry.)

Supplementary References

1. D. Zhu et al., Human cytomegalovirus reprogrammes haematopoietic progenitor cells into immunosuppressive monocytes to achieve latency. Nat Microbiol 3, 503-513 (2018).

2. E. Van Damme et al., Glucocorticosteroids trigger reactivation of human cytomegalovirus from latently infected myeloid cells and increase the risk for HCMV infection in D+R+ liver transplant patients. J Gen Virol 96, 131-143 (2015).

3. C. M. O'Connor, E. A. Murphy, A myeloid progenitor cell line capable of supporting human cytomegalovirus latency and reactivation, resulting in infectious progeny. J Virol 86, 9854-9865 (2012).

4. E. Poole, J. C. H. Lau, J. Sinclair, Latent infection of myeloid progenitors by human cytomegalovirus protects cells from FAS-mediated apoptosis through the cellular IL-10/PEA-15 pathway. J Gen Virol 96, 2355-2359 (2015).

5. E. Poole et al., An iPSC-Derived Myeloid Lineage Model of Herpes Virus Latency and Reactivation. Front Microbiol 10, 2233 (2019).

6. S. Straschewski et al., Human cytomegaloviruses expressing yellow fluorescent fusion proteins--characterization and use in antiviral screening. PLoS One 5, e9174 (2010).

7. C. Sinzger et al., Modification of human cytomegalovirus tropism through propagation in vitro is associated with changes in the viral genome. J Gen Virol 80 (Pt 11), 2867-2877 840 (1999).

8. K. L. Sampaio, Y. Cavignac, Y. D. Stierhof, C. Sinzger, Human cytomegalovirus labeled with green fluorescent protein for live analysis of intracellular particle movements. J Virol 79, 2754-2767 (2005).

9. S. E. Jackson et al., Latent Cytomegalovirus (CMV) Infection Does Not Detrimentally Alter T Cell Responses in the Healthy Old, But Increased Latent CMV Carriage Is Related to Expanded CMV-Specific T Cells. Front Immunol 8, 733 (2017).

10. M. W. Pfaffl, A new mathematical model for relative quantification in real-time RT-PCR. Nucleic Acids Res 29, e45 (2001).

11. H. M. Parry et al., Cytomegalovirus viral load within blood increases markedly in healthy people over the age of 70 years. Immun Ageing 13, 1 (2016).

12. H. Keren-Shaul et al., MARS-seq2.0: an experimental and analytical pipeline for indexed sorting combined with single-cell RNA sequencing. Nat Protoc 14, 1841-1862 (2019).

13. E. Van Damme, M. Van Loock, Functional annotation of human cytomegalovirus gene products: an update. Front Microbiol 5, 218 (2014).

14. K. Nightingale et al., High-Definition Analysis of Host Protein Stability during Human Cytomegalovirus Infection Reveals Antiviral Factors and Viral Evasion Mechanisms. Cell Host Microbe 24, 447-460.e411 (2018).

15. J. Vandesompele et al., Accurate normalization of real-time quantitative RT-PCR data by geometric averaging of multiple internal control genes. Genome Biol 3, RESEARCH0034 (2002).

16. L. Shan et al., Killer cell proteases can target viral immediate-early proteins to control human cytomegalovirus infection in a noncytotoxic manner. PLoS Pathog 16, e1008426 (2020).

17. S. Omoto, E. S. Mocarski, Cytomegalovirus UL91 is essential for transcription of viral true late (γ2) genes. J Virol 87, 8651-8664 (2013).

18. A. K. L. Cheung, Y. Huang, H. Y. Kwok, M. Chen, Z. Chen, Latent human cytomegalovirus enhances HIV-1 infection in CD34. Blood Adv 1, 306-318 (2017).

19. M. A. Dawson et al., Inhibition of BET recruitment to chromatin as an effective treatment for MLL-fusion leukaemia. Nature 478, 529-533 (2011).

20. H. M. Coleman et al., Histone modifications associated with herpes simplex virus type 1 genomes during quiescence and following ICP0-mediated de-repression. J Gen Virol 89, 68-77 (2008).

21. C. M. Mastroianni et al., Cytomegalovirus encephalitis in two patients with AIDS receiving ganciclovir for cytomegalovirus retinitis. J Infect 29, 331-337 (1994).

22. I. J. Groves, J. H. Sinclair, Knockdown of hDaxx in normally non-permissive undifferentiated cells does not permit human cytomegalovirus immediate-early gene expression. J Gen Virol 88, 2935-2940 (2007).

23. M. Nevels, C. Paulus, T. Shenk, Human cytomegalovirus immediate-early 1 protein facilitates viral replication by antagonizing histone deacetylation. Proc Natl Acad Sci U S A 101, 17234-17239 (2004).